AD_____

Award Number: DAMD17-99-1-9315

TITLE: Discovery of DNA Binding Anticancer Drugs That Target Oncogenic Transcription Factors Associated with Human Breast Cancer

PRINCIPAL INVESTIGATOR: Terry A. Beerman, Ph.D.

CONTRACTING ORGANIZATION: Health Research, Incorporated
Buffalo, New York 14263

REPORT DATE: October 2002

TYPE OF REPORT: Final

PREPARED FOR: U.S. Army Medical Research and Materiel Command
Fort Detrick, Maryland 21702-5012

REPORT DOCUMENTATION PAGE

Form Approved
OMB No. 074-0188

1. AGENCY USE ONLY (Leave blank)	2. REPORT DATE	3. REPORT TYPE AND DATES COVERED
	October 2002	Final (15 Sep 99 - 14 Sep 02)

4. TITLE AND SUBTITLE
Discovery of DNA Binding Anticancer Drugs That Target Oncogenic Transcription Factors Associated with Human Breast Cancer

5. FUNDING NUMBERS
DAMD17-99-1-9315

6. AUTHOR(S)
Terry A. Beerman, Ph.D.

7. PERFORMING ORGANIZATION NAME(S) AND ADDRESS(ES)
Health Research, Incorporated
Buffalo, New York 14263

E-Mail: terry.beerman@roswellpark.org

8. PERFORMING ORGANIZATION REPORT NUMBER

9. SPONSORING / MONITORING AGENCY NAME(S) AND ADDRESS(ES)
U.S. Army Medical Research and Materiel Command
Fort Detrick, Maryland 21702-5012

10. SPONSORING / MONITORING AGENCY REPORT NUMBER

11. SUPPLEMENTARY NOTES

12a. DISTRIBUTION / AVAILABILITY STATEMENT
Approved for Public Release; Distribution Unlimited

12b. DISTRIBUTION CODE

13. ABSTRACT *(Maximum 200 Words)*

This proposal is designed to develop sequence specific DNA binding polyamides as an approach for specifically inhibiting Her2/neu expression, a gene that is over expressed in human breast cancers. The approach is to design polyamides that are optimized for targeting the binding of ESX a transcription factor which up regulates Her2/neu by binding to its consensus site within the Her2/neu promoter. Active agents are tested for their ability to inhibit Her2/neu expression in both cell free and cellular systems. A number of polyamides were identified as being effective inhibitors of ESX complex formation and their ability to block complexes was analyzed in detail. None of the agents were effective at preventing expression in cells. A series of fluorescently labeled polyamides representing structural diverse compounds were tested for their ability to localize in the nucleus of live cells. No agent was found to localize in the nucleus even at relatively high concentrations or for incubations times up to several days. Studies are underway to develop a new generation of polyamides that posses not only the ability to effectively target the HER2/neu promoter under cell free conditions but also to function effectively on nuclear DNA targets in intact cells.

14. SUBJECT TERMS	15. NUMBER OF PAGES
breast cancer, polyamides, DNA binding, transcription, oncogenic	81
	16. PRICE CODE

17. SECURITY CLASSIFICATION OF REPORT	18. SECURITY CLASSIFICATION OF THIS PAGE	19. SECURITY CLASSIFICATION OF ABSTRACT	20. LIMITATION OF ABSTRACT
Unclassified	Unclassified	Unclassified	Unlimited

Table of Contents

(4). INTRODUCTION

The project is designed to develop sequence specific DNA binding agents that can preferentially target the ETS transcription factor ESX that is involved in aberrant upregualtion of HER2/neu in human breast cancer. The approach is to utilize DNA minor groove binding agents (polyamides) synthesized by our collaborator Dr. Peter Dervan to block the association of ESX with its consensus binding site within the HER2/neu promoter. Since polyamides have the ability to recognize DNA at the sequence level, it should be possible to design agents that would strongly compete with ESX for its DNA binding site within the promoter. Successful compounds will be assessed for their ability to inhibit ESX regulated gene expression under cell-free conditions to document that blocking the complex also inhibits transcription. Active compounds will be tested for their ability to preferentially block ESX regulated expression of HER2/neu in cells as well as for general biological activity. Since this is a first phase for developing polyamides as specific inhibitors of transcription factor/DNA complexes, early experiments are designed to test the feasibility of the concept and to uncover approaches which would insure that compounds are specific as DNA targeting agents and that can function in cells.

(5). BODY [1]

Overview. The mission of the research was to develop sequence specific DNA binding polyamides that could preferentially inhibit association of the ESX transcription factor with its binding site on the HER2/neu promoter. The first phase of the study was to evaluate a number of polyamides synthesized to bind to different parts of the ESX DNA binding site on the promoter to determine what type of DNA binding motifs lead to effective disruption of ESX/DNA complexes. Once compounds were found that block complex formation further modifications were to be made to try and enhance the inhibition while new studies were to be undertaken to determine the potential of the ESX complex inhibitors to block expression under cell free conditions. During the next phase, refinements were to be made in selecting agents that work as both complex inhibitors as well as being capable of inhibiting cell free gene expression along with an evaluation of compound activity in cells.

The scenario described above was written into a three year study with compounds functioning in cells being emphasized in the second and third years. Since the funding was limited to two years, we did speed up the whole cell assessment by examining some of the effective cell free inhibitors in cellular assays during the first year. The rational was that the shortened funding period would may not allow allowed sufficient time to develop agents that could function in cells if cell–free inhibitors were not also effective in a cellular environment. As will be described below this was prudent in that the promising lead compounds developed from the cell free analysis turned out to not function well in cells. This prompted us to diminish the emphasis on optimizing polyamides as ESX complex inhibitors in the cell free studies and expand our efforts towards finding ways of optimizing these agents for cellular activity. Essentially the task became one of developing polyamides as effective and selective transcription factor inhibitors while simultaneously looking for ways to optimize their pharmacological activity in a cellular environment. While initial evidence based upon uptake studies suggested that polyamides were generally capable of entering mammalian cells and binding to nuclear DNA, more detailed assessments negated these early findings. At this point a sustained effort has been made to understand the basis for the lack of cellular uptake and to explore ways to modify polyamides to make them functional in a whole cell setting. The

[1] This proposal received a no cost extension ($10,500) in Oct. of 2002. Since most of the grant funds have already been expended, the previous report covers much of what is in this final report.

integration of these efforts within the statement of work periods is provided below.

AIM 1 Identification of modular polyamide DNA minor groove binders that interfere with the binding of ESX to HER2/neu promoter DNA in cell-free assays: This aim was covered in the past reports which included a paper describing polyamides that can block ESX/DNA complexes.

AIM 2 Effects of modular polyamide DNA minor groove binders on ESX regulated expression of the HER2/neu proto-oncogene: Part of this aim was covered in past reports and findings where included in a paper that assessed the ability of polyamides to block HER2/neu expression under cell free conditions. Also in the previous reports, we eluded to initial studies to test the effectiveness of polyamides to block HER2/neu expression in intact cells. Summarizing from the past years, we found that unlike the cell free expression studies, we could find no evidence of inhibition of HER2/neu in a variety of human breast cancer cell lines as well as other cell types such AS NIH3T3, BSC-1 and HeLa cells. We went on to document that using conventional DNA binding agents including several that bind like polyamides to the DNA minor groove, distamycin, chromomycin, Hoechst 33258 and hedamycin were able to inhibit ESX/DNA complexes and gene expression under cell free conditions and that HER2/neu expression was also inhibited in intact cells. Moreover, unlike the polyamides each drug was able to inhibit cell growth. At the same time, the polyamides were shown to be much more potent DNA binding agents than these conventional compounds suggesting that whole cell activity of polyamides was somehow compromised. While the conventional agents proved to be effective in cells, the data also suggested that their effects on expression were not specific and were more likely due to induction of cytotoxicity than to targeting the HER2/neu promoter.

At this point, we began a rigorous assessment of polyamide uptake into cells, since the preliminary evidence that uptake was observed was inconsistent with a lack of biological activity in cells including lack of effect on gene expression or cytotoxicity. These studies included examination of uptake and localization of a series of fluorescently labeled polyamides into live cells. Experiments were also initiated to evaluate whether modifications could be made to the treatment conditions to enhance cellular uptake. Selected finding from these studies are provided below and include representative data (figures and table numbers are not consecutively numbered):

Additional studies. At this point we realized the necessity of focusing more on the factors that influence polyamides to block expression than those that would enhance their ability to block complex formation (months 7-12) since the later was successful while the former was weaker than expected. While we had intended to carry out primarily cell free expression assays during months 7-12, we felt it was important for several reasons to carry out a preliminary assessment of polyamide activity as inhibitors of HER2/neu expression in cells although these experiments were not to begin until months 19-24. Most importantly, it was necessary to know, if like in the cell-free assessment, activity would be lower than anticipated for polyamide activity as inhibitors of HER2/neu expression in intact cells. Also since the funding period was reduced to two years, it would be even more critical to develop polyamide transcription inhibitors early on as there would be less opportunity for discovery of agents that can function in intact cells if we delayed doing whole cell evaluations until the 19-24 months. Selected finding from these studies are provided below and include representative data where appropriate:

Cellular uptake and localization of MGBs and 22 in live SK-Br-3 cells. The lack of whole cell activity of polyamide **2** (see structure in Fig. 29) which was one of mist potent cell-free inhibitors of ESX/DNA complexes would be explainable by the fact that mammalian cells may not be readily permeable to polyamides. While a published paper does report polyamide effects on transcription in cells, it was limited to one cell type and one type of polyamide so it is possible that the findings are not readily applicable to other compounds or cell types. At this point we evaluated the degree of permeability of mammalian cells to polyamides using a modified **2** provided by the Dervan laboratory which contained an attached fluorescent probe (BODIPY). This compound named **22** (see structure in Fig. 29) was evaluated for its ability to enter mammalian cells and also its localization in cells was determined. Our initial assessment reported previously that the compound was well taken up by the nucleus was not correct. It turns out that using standard fixation procedures such as methanol treatment to fix cells for microscopic examination somehow altered the uptake pattern. This was surprising given that such fixation does not alter localization of conventional minor groove binding agents and there use is common practice in many types of localization studies. Nevertheless the data comparing uptake of **22** into live cells (essentially

compound is added and after indicated incubation time cells are removed from the incubator and pictures are immediately taken of the unfixed cells to determine the distribution of the fluorescent signal) demonstrates that bright nuclear localization signals are only observed in the methanol fixed cells. Extensive analysis has confirmed that **22** over a wide range of concentrations and incubation times is unable to reach the nucleus when the analysis is carried out with live cells. Several cell lines including human breast cell lines SKBR3, HeLa, NIH3T3 all gave similar findings. While the data was disappointing, it provided an explanation of why we were seeing such little biological activity from polyamide compounds.

Representative data

To assess if cellular uptake and localization are potential barriers to PA activity in cells, SK-Br-3 cells were grown on glass cover slips and exposed to **22** at 0.5 mM for 1 hour. To compare **22**'s uptake with other MGBs known to localize to the nucleus and bind DNA, SK-Br-3 cells were also exposed to Hoechst 33342, Hoechst 33258 or DAPI at 0.5 mM for 1 hour. Following exposure cells were then washed several times with PBS, to remove excess drug/ligand, and placed cell side down on a slide with spacers[11]. In addition to fluorescence images, bright field images were captured for determination of cellular localization. Figure 30 (A-D) shows representative images with the bright field on top and the corresponding fluorescence on the bottom. These images demonstrate the ability of each of the classical MGBs to reach the nucleus, albeit to different degrees. Semi-quantitative analysis and determination of each image's integrated optical density (IOD, Table 6) showed superior uptake of Hoechst 33342 in SK-Br-3 cells when compared with Hoechst 33258 and DAPI, nearly 10X and 20X, respectively (Figure 30B and 30C, respectively). However, for **22** there was no visible fluorescence in either the nucleus or the cytoplasm and semi-quantitative analysis revealed no detectable fluorescence (Figure 30 D).

While **22** is a MGB it is structurally different than the conventional compounds including being larger, it is conceivable that this agent requires more time for uptake into the cells. Figure 31A illustrates representative time course study evaluations of **22** and the enhanced detection of discrete punctate staining in the cytoplasm with increased ligand exposure time. These staining regions were compared to staining using Lysotracker, which's used to identify lysosomes. While we were able to show that some of **22** does reside in

[11] The presence of the spacers prevents the weight of the cover slip from squashing the cells and provides sufficient time for a minimal visualization and image capture of each agent's localization in the live cells.

liposomes it was never more than a small percentage of the expected total signal if substantial compound were visible in the cytoplasm. Similarly, we found indications that a very small amount of **22** was associated with mitochondria (based upon co-localization studies using a mito tracker co stain). For comparison purposes, Fig. 42 provides the localization profile of SK-BR-3 cells treated with 0.5UM **22** at the indicated times prior to fixation with solvent. Note that almost all the fluorescent signal is nuclear in contrast to the live cell images in Fig. 31 A.

A second polyamide **3** that was used in our original study of the effects of polyamides on HER2/nue expression in cell free systems (reported on in the last report which included a publication (Chiang, S-Y., Burli, R., Scott, G., Gawron L., Benz, C., Dervan, P., Beerman T. Targeting the ESX Binding Site of the HER2/neu Promoter with Pyrrole-Imidazole Polyamides. J. of Biol. Chem. 275:24246-24254, 2000) was also tagged with fluorescent Bodipy to create **33**. The uptake studies were similar to what was observed with **22** in that only when cells were fixed did we see a strong fluorescent signal in the nucleus while live cells showed minimal signal levels comparable to **22**. One potentially interesting difference was noted in that in the fixed cells the nuclear localization pattern for **33** was distinct from what was observed with **22**. In contrast to **22** which appears to localize throughout the nucleus and is likely associated with chromatin structures, **33** resides mainly on the inner side of the nuclear membrane.

Further evaluation of mammalian cell permeability to polyamides.

At this point we turned our attention to determining the generality of our findings and began to study uptake and localization of a series of polyamides with varying structural modifications. This was partly driven by the unexpected differences in localization between **22** and **33**. These two compounds are structural quite similar in that they are made of imidazole and pyrrole rings with **22** having ten rings and **33** eight and the latter has an internal beta alanine. To further evaluate whether ring composition or beta alanine structure could effect uptake in live cells a series of compounds were synthesized each containing a fluorescent tag (most contained Bodipy tag but one was made with Tamra). The structures varied in ring composition and number as well as number of beta alanines as shown below in the tables (Py – pyrrole and Im – imidazole). A schematic of the dye structures is shown in Fig. 61.

Agent	# of rings	Im vs Py	# of β-alanines
PA33	8		
Dye 4	8		

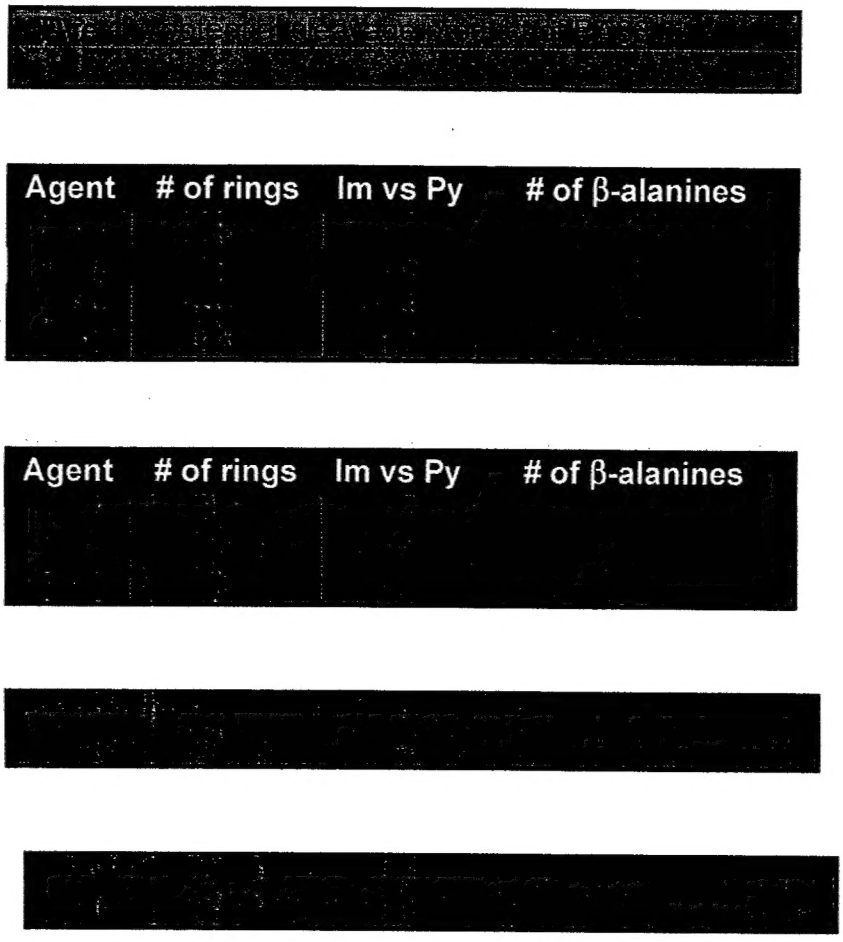

Representative data.

Cellular uptake and localization of Dye 1-7 in live SK-Br-3 cells.

SK-Br-3 cells were grown on cover slips and exposed to Dyes 1-7 at 0.5 mM for 1 or 24 hours. Following exposure cells were washed several times with PBS and placed cell side down on a slide. In addition to fluorescence images, bright field images were captured for determination of cellular localization. Figure 62 shows representative images demonstrating no detectable fluorescence following a 1-hour treatment with any Dye. The lack of detectable staining was similar to results obtained at the 1-hour time point for both **22** and **33**. At the 24-hour time point each Dye showed detectable fluorescence as seen in Figure 62. Dye 1, the potential cleavage product of **33**, showed punctate cytoplasmic staining that clearly avoids the nucleus (Figure 62A). Similarly, Dye 2 showed punctate cytoplasmic staining although it's staining was slightly less than that seen with Dye 1 (Figure 62B). In contrast with the punctate cytoplasmic staining seen with Dyes 1 and 2, Dye 3 appears to localize at the plasma membrane (Figure 62C). Dye 4 on the other hand demonstrated diffuse

cytoplasmic staining which clearly avoided the nucleus (Figure 62D). Dye 5, Figure 62E, showed punctate cytoplasmic staining but also had a few sites that were larger and more intense. Similarly, Dye 6 also demonstrated these isolated intense punctate cytoplasmic staining (Figure 62F). Dye 7 (Figure 62G) behaved similarly to **22** with punctate cytoplasmic staining. The data is summarized in Table 9 which provides estimates of optical density over time obtained in cells for each compound. In contrast each of dyes when examined in fixed cells, was able to reach the nucleus with the exception that the fragment compounds 1 and 2 which showed very little uptake.

Studies carried out during the extension period.

Currently, we are pursuing whether liposome-facilitated delivery of the PAs results in increased uptake. The desired endpoint is nuclear fluorescence, which would indicate co-localization of the agents with DNA. In preliminary experiments using **Dye 7**, the effectiveness of different commercially available liposome formulations was compared. Lipofectamine, a polycationic and neutral lipid mixture from InVitrogen/Life Technologies, and PolyFect, a spherical dendrimer possessing charged amino groups from Qiagen, were selected for initial analyses. Both reagents are commonly used for transfection of a wide range of cell lines. **Dye 7** was incubated with carrier DNA before being combined with liposomes according to the manufacturer's instructions. The carrier DNA chosen for these experiments was pFosLuc. This plasmid contains the full-length human c-fos promoter, a sequence containing A/T rich sites to which **Dye 7** can potentially bind. The liposome/DNA/PA mixture was applied to NIH3T3 cells grown on cover slips. Total treatment time, as well as **Dye 7**, DNA, and liposome concentrations, were systematically varied in an effort to optimize treatment conditions. DNA was omitted from some samples to determine whether its inclusion was necessary for **Dye 7** uptake. Following incubation with the liposome mixtures, the coverslips were pried from their cell culture dishes and mounted in phosphate buffered saline before being viewed immediately on the epifluorescence microscope. Under these conditions, the cells remain viable for a short time. Under these conditions, there was no evidence of enhanced **Dye 7** uptake. A continuation of these initial studies are being carried out with funding from other sources.

(6). KEY RESEARCH ACCOMPLISHMENTS

- Determined that polyamides may not have ready access to the cell nucleus when given to intact mammalian cells and that the lack of uptake is wide spread

amongst cell types. Thus, polyamide appear to have great potential to target specific regions of DNA at the sequence level and as such can effectively disrupt transcription factor DNA complexes, there limited ability in entering the cell nucleus limits there pharmacological promise. Based upon our research effort is now being put forth to design polyamide with the ability to be taken up in mammalian cells.

•Determined that the HER2/neu model system is well suited to showing that conventional DNA binding agents can target and block HER2/neu expression in intact cells.

• Based upon structure activity analysis of a series of polyamides, an inability to enter the cell nucleus appears to be a common feature although the uptake patterns vary with polyamide structure.

• Small amounts of polyamide were found to co-localize within lysosomes but not mitochondria.
• Standard liposome formulations were unable to improve polyamide uptake into mammalian cells.

(7). REPORTABLE OUTCOMES

• Submission of a manuscript documenting the utilization of the HER2/neu model system for evaluating targeting of the promoter using conventional DNA binding agents was not successful. Subsequently, new data was added and an updated version will be submitted in early 2003.
Leslie, S., Scott, G., Benz, C., and Beerman T.A. Effect of sequence preference DNA binding drugs on ESX transcription factor binding to the HER2/neu promoter and gene expression. For submission in 2003.

(8). CONCLUSIONS.

Based upon our rather extensive analysis of polyamide uptake and localization in live cells, it appears that the inability of these agents to reach the nucleus is fairly universal. Despite varying the ring composition in both ratios of pyrroles to imidazoles and well as the number of rings, no compound demonstrated strong nuclear localization compared to classical DNA minor groove binding agents. Nor was the lack of uptake restricted to a particular cell type. Future studies in the development of these compounds will emphasize more radical modification of the polyamide backbone to see whether agents can

be developed that maintain effective DNA binding but also are permeable to cells.

A second approach underway in our laboratory is to use liposomes to transport the compounds past the plasma membrane. To date this later approach has not been successful and it is likely that specific liposome formulations will be needed to optimize encapsulation of the polyamides and to allow there release once past the plasma membrane.

(9). REFERENCES.

References are provided in the accompanying paper provided in Appendix A.

(10). APPENDICES.

A. Manuscript.
B. Unpublished data

APPENDIX A

Manuscript.
Leslie, S., Scott, G., Benz, C., and Beerman T.A. Effect of sequence preference DNA binding drugs on ESX transcription factor binding to the HER2/neu promoter and gene expression.. Molecular Pharmacology, revised for 2003.

Previous publication.
Chiang, S-Y., Burli, R., Scott, G., Gawron L., Benz, C., Dervan, P., Beerman T. Targeting the ESX Binding Site of the HER2/neu Promoter with Pyrrole-Imidazole Polyamides. J. of Biol. Chem. 275:24246-24254, 2000

Personal involved on project

Barb Dziegielewska (graduate student)
Loretta Gawron (technision)
Xia Yin (post doc)
Michael Smith (part time lab helper)
Matthew Feldman (part time lab helper
Tara Felmet (part time lab helper
Brian Philips (post doc)
Yong-Dong Wang (post doc)

APPENDIX B

Unpublished data

APPENDIX B

Unpublished data

Figure 29

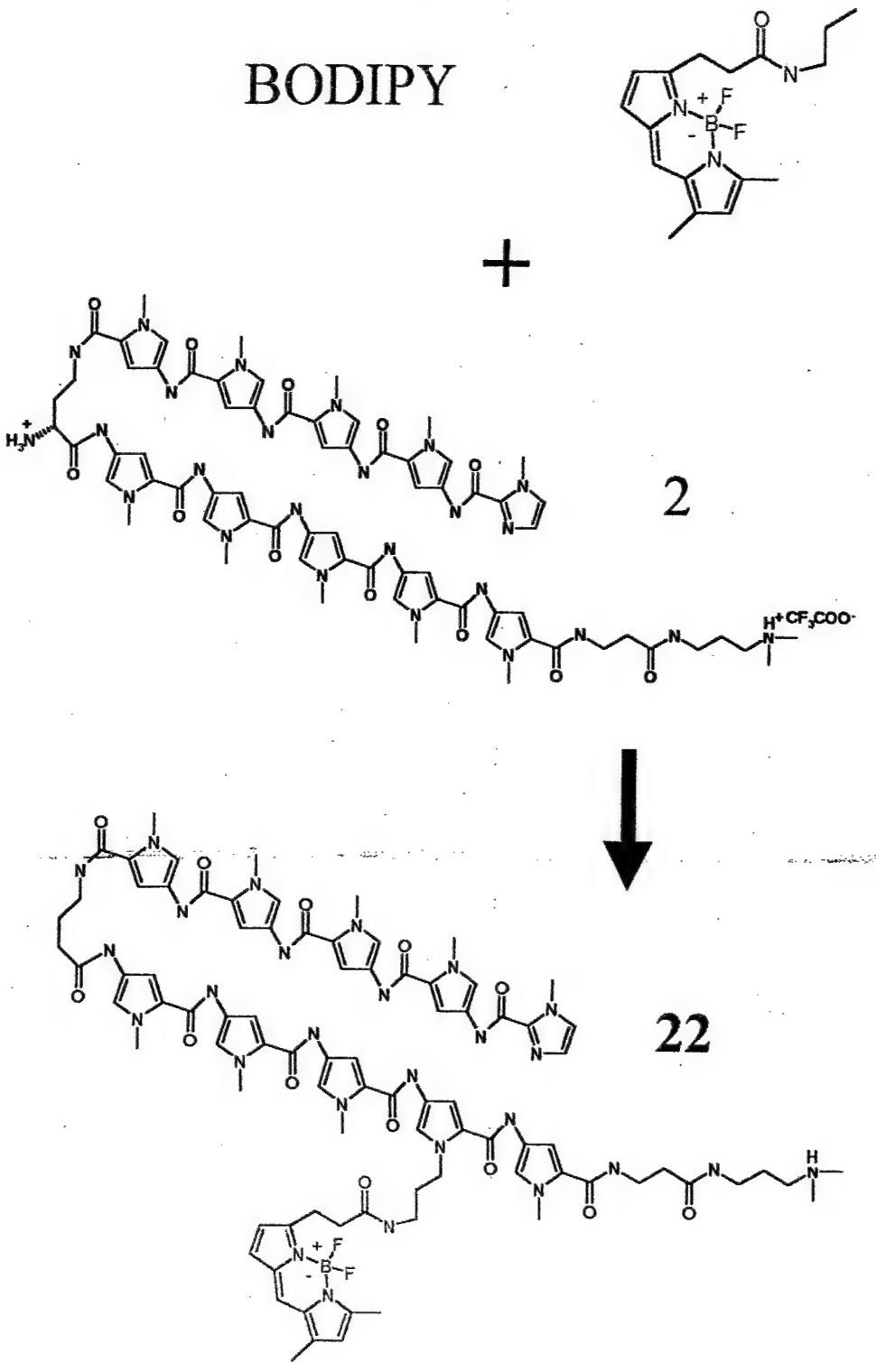

Figure 30: Determination of the subcellular localization of naturally fluorescent MGBs and the fluorescently labeled PA, 22, in live cells. SK-Br-3 cells were grown on cover slips and treated with indicated drug at 0.5 μM for 1 hour. Cells were then washed in room temperature PBS, removed and placed cell side down on a slide and visualized by epifluorescence microscopy. Each figure section contains a bright field image (upper panel) and the corresponding fluorescent image (lower panel). ***A***, Hoechst 33342; ***B***, Hoechst 33258; ***C***, DAPI; ***D***, **22**. *Imaging system,* SPOT RT. *Camera exposure,* 100 msec. *Scale bar*, 20 μm.

Figure 30A

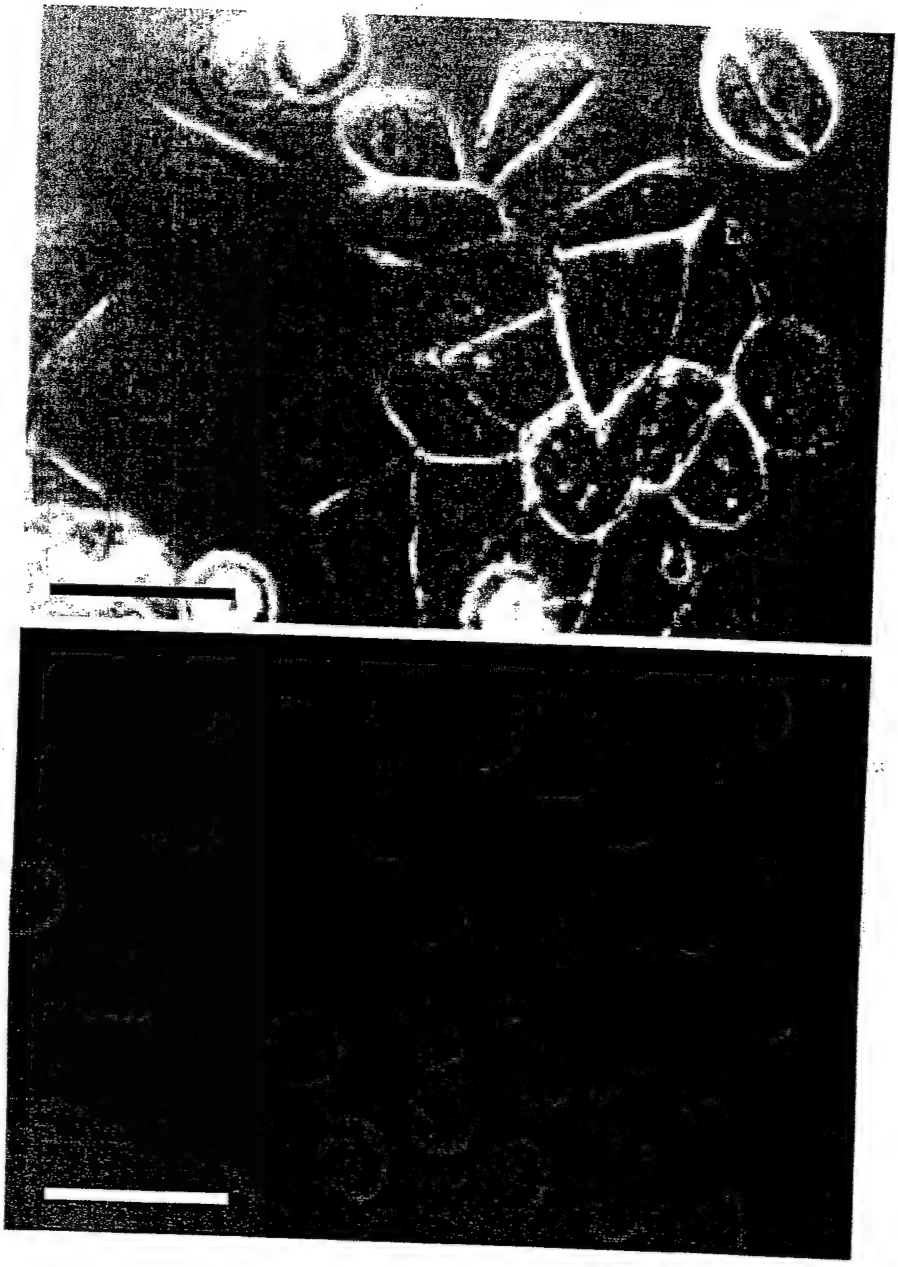

Figure 30B

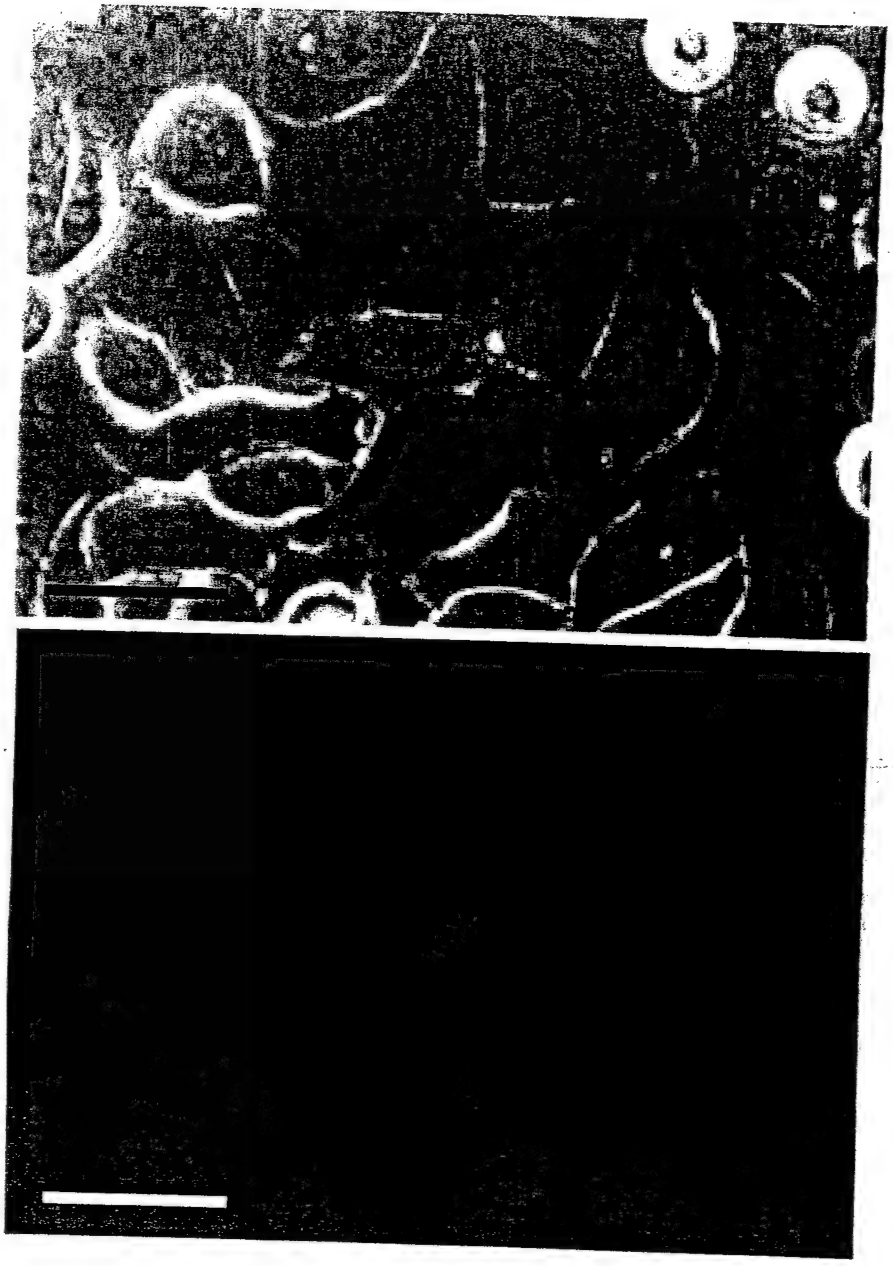

Figure 30C

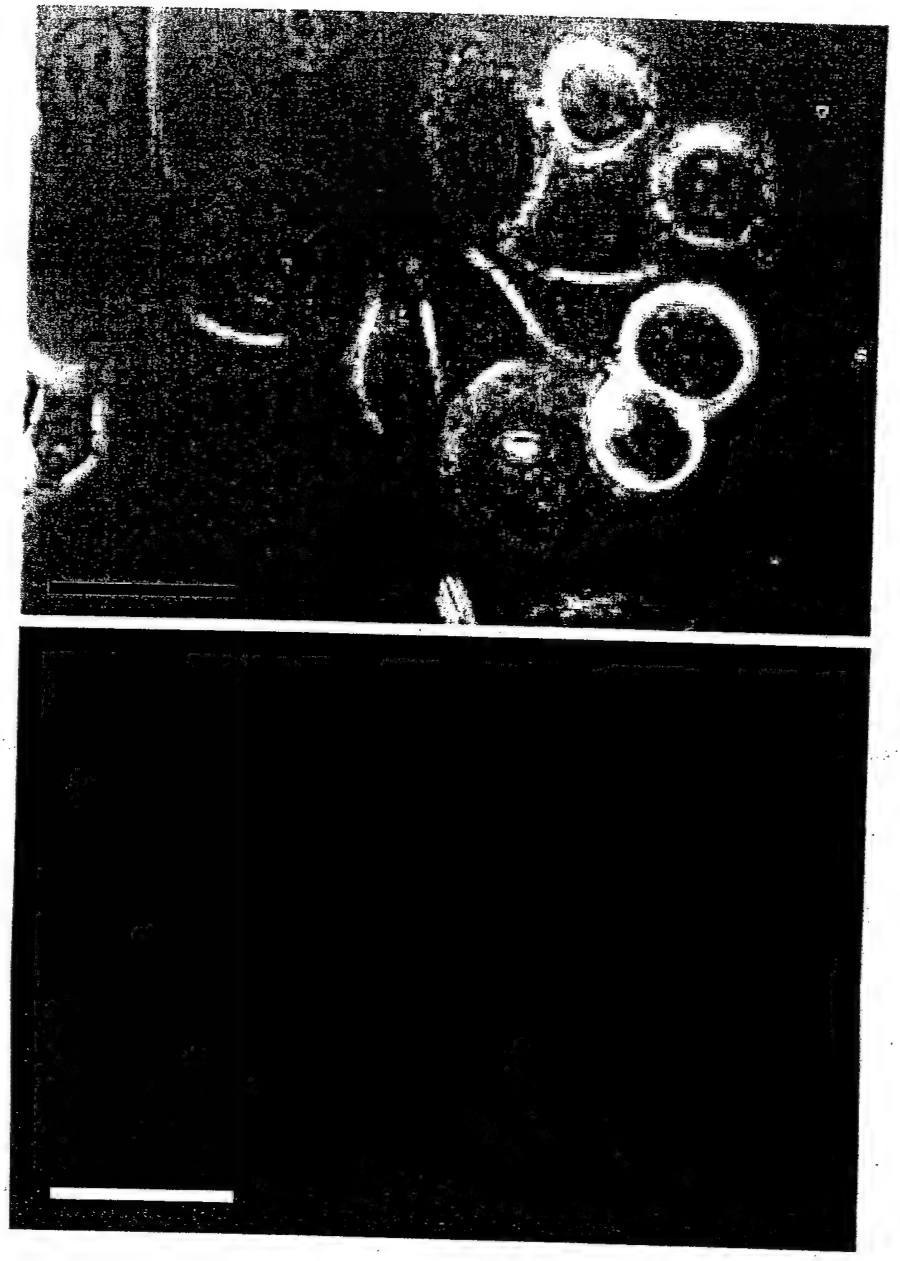

Figure 30D

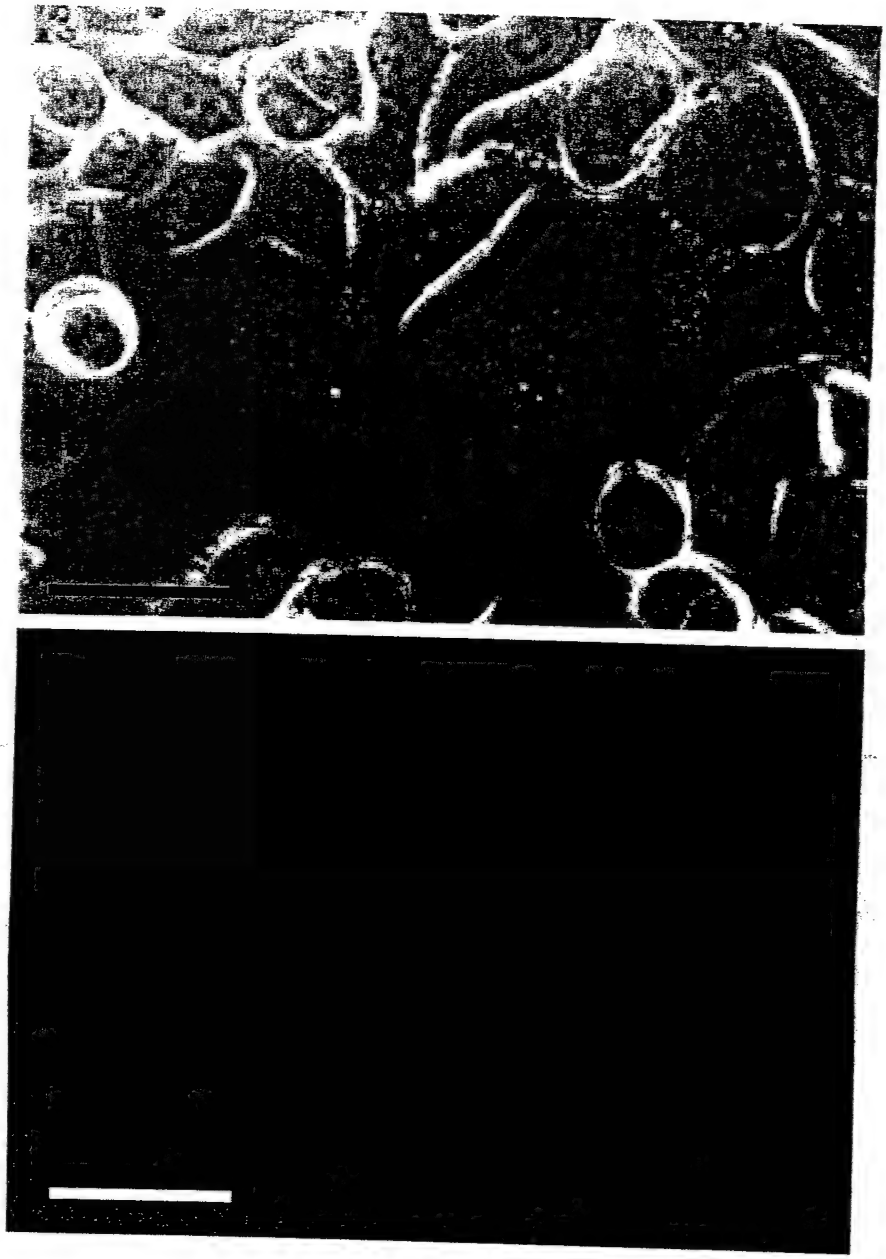

Table 6: Results of semi-quantitative analysis of fluorescence intensity.

Each of the fluorescence images in Figures 30 and 33 were analyzed using Image Pro Plus. Briefly, the integrated optical density (area multiplied by pixel intensity) for each cell within an image was determined. These IOD values were then averaged using the number of cells within the image to give an "image average IOD".

Table 6

Drug/Ligand	IOD
Hoechst 33342	2452
Hoechst 33258	212
DAPI	128
22	4
22 + CL	45

Figure 31: Uptake and localization of Hoechst 33342 and 22 over time.

SK-Br-3 cells were grown on cover slips and treated with indicated drug at 0.5 μM for specified time points. Cells were then washed in room temperature PBS, removed and placed cell side down on a slide and visualized by epifluorescence microscopy. Each figure section contains a bright field image (upper panel) and the corresponding fluorescent image (lower panel) with the exception of ***C***, which contains a merged image. ***A***, **22**; ***B***, Hoechst 33342. ***C*** is a close up of a single cell from 48-hour time point in ***A*** showing the localization of **22**'s fluorescence (middle panel) with vesicles in the bright field image (top panel). *Imaging system,* SPOT RT. *Camera exposure*, 2 sec for ***A*** and 500 msec for ***B***. *Scale bar*, 20 μm.

Figure 31A

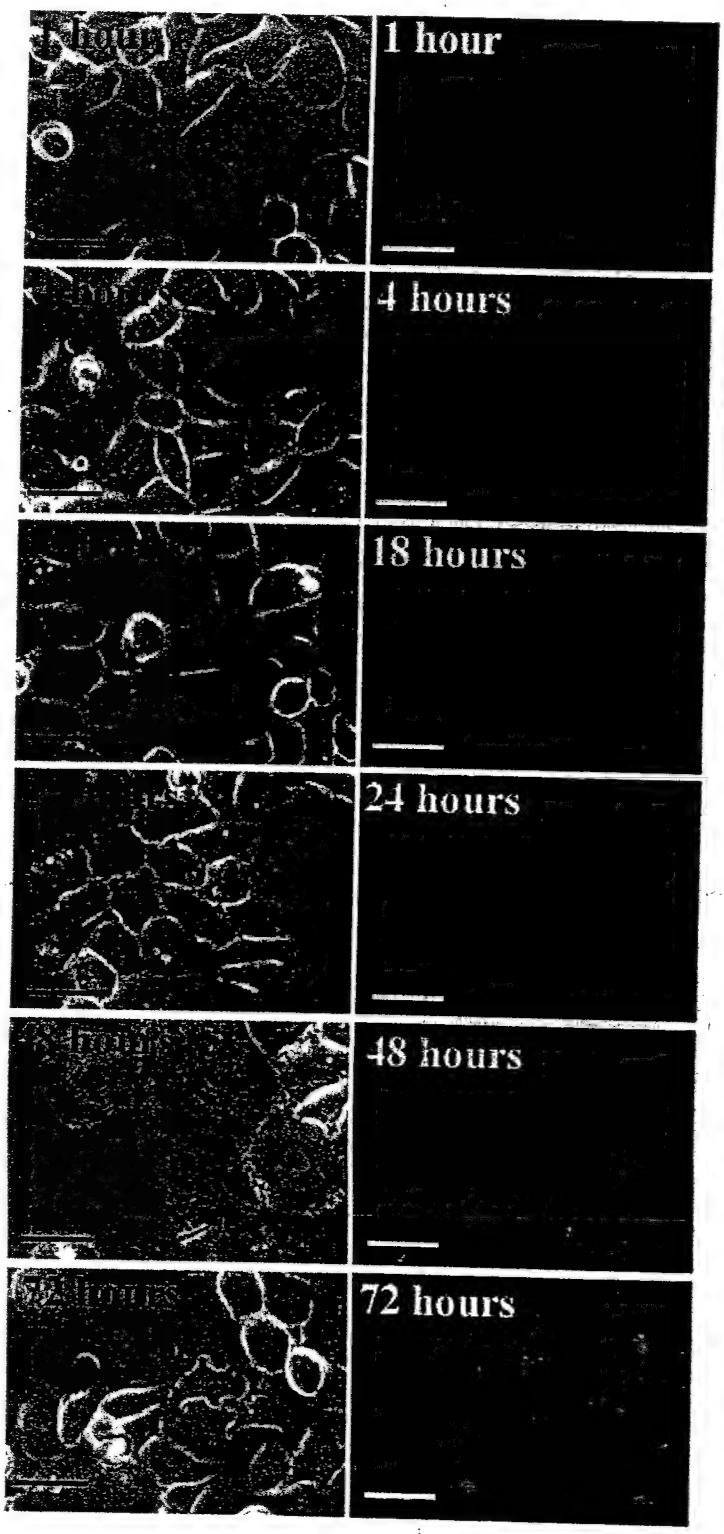

Figure 31B

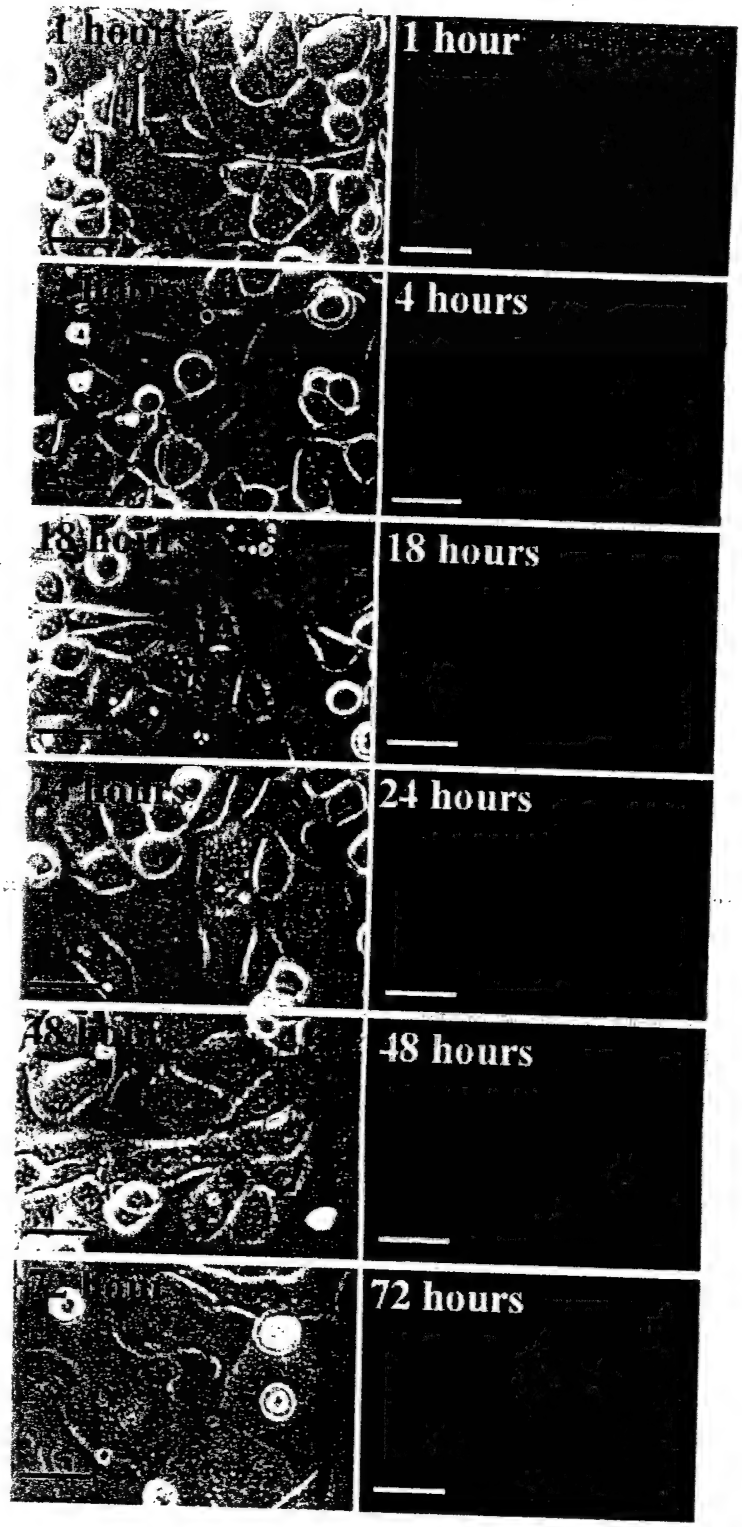

Figure 42

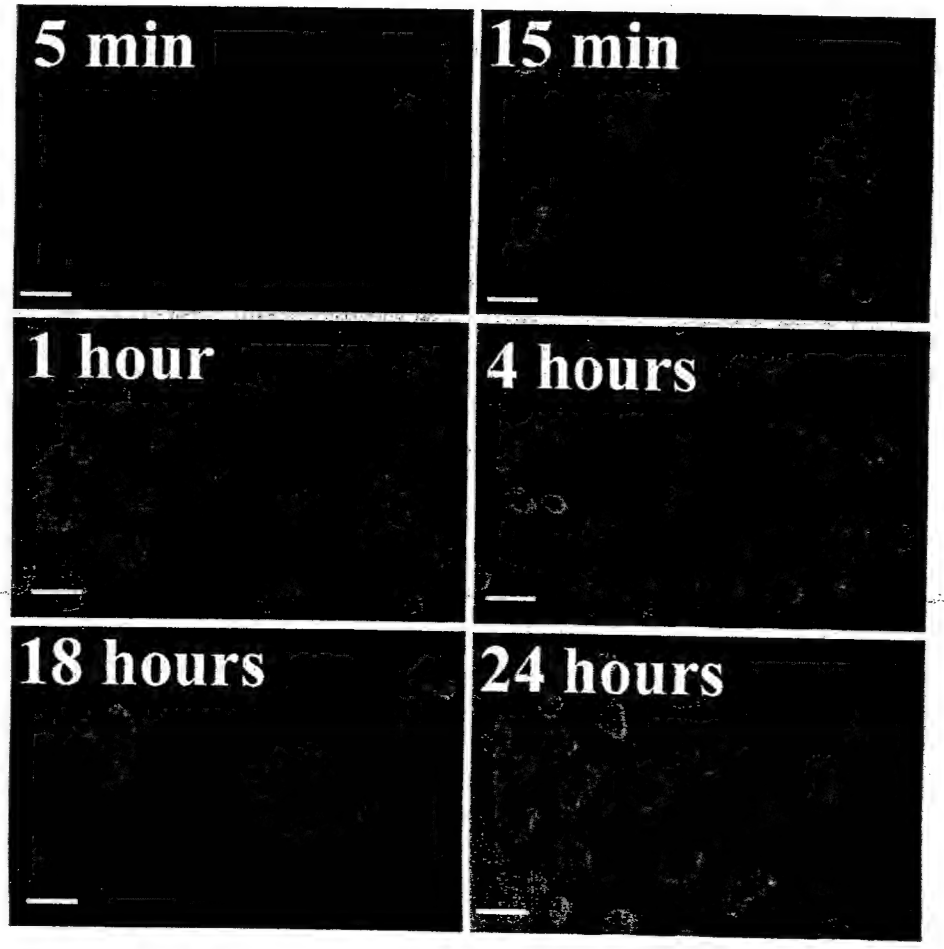

Figure 42: Cellular uptake of 22 over time. SK-Br-3 cells were treated with 0.5 μM of 22 at the indicated times points prior to fixation. *Fixative*, acetone. *Imaging system*, Kodak EOS-DCS5. *Exposure time*, 2 sec. *Scale bar*, 50 μm.

Figure 61: Structures of rationally designed Dyes. Dye 1 is the potential cleavage product of **33**. Dye 2 is a PA similar in ring number and composition as distamycin. Dye 3 is a combination of top arm of **33** and the bottom arm of **22**. Dye 4 and Dye 5 have the same ring number but different ring composition. Dye 6 has multiple structural changes compared with **22** and Dye 3. Dye 7 has the same PA backbone as **22** but contains Tamra fluorescent tag rather than Bodipy. Their chemical structures can be found in Appendix A.

Figure 61

Dye 1

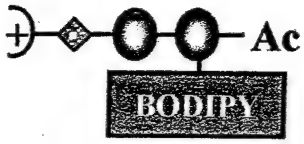

Dye 2

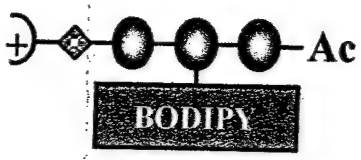

Dye 3

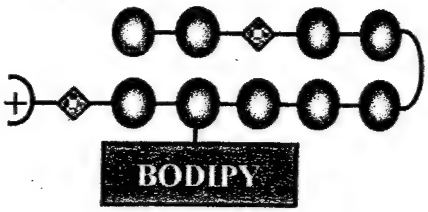

Dye 4

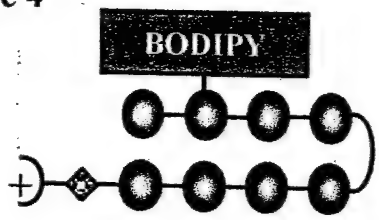

Dye 5

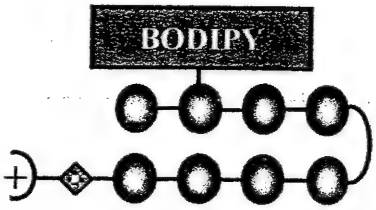

Dye 6

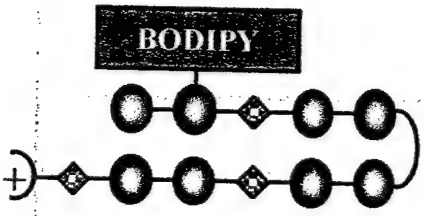

Dye 7

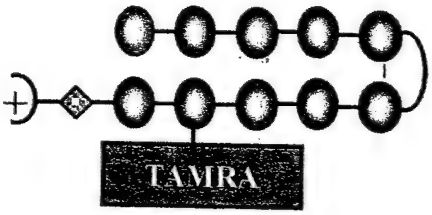

Figure 62: Dye localization in live cells at short periods of time. SK-Br-3 cells grown on cover slips were treated for 1 hour with each Dye at 0.5 μM. Cells were washed twice in PBS, placed cell side down on slides and viewed by epifluorescence microscopy. The left side contains the bright field images while the right side is the corresponding fluorescence image with the Dye indicated on the images. *Imaging system*, SPOT RT. *Camera exposure*, 2 sec. *Scale bar*, 20 μm.

Figure 62

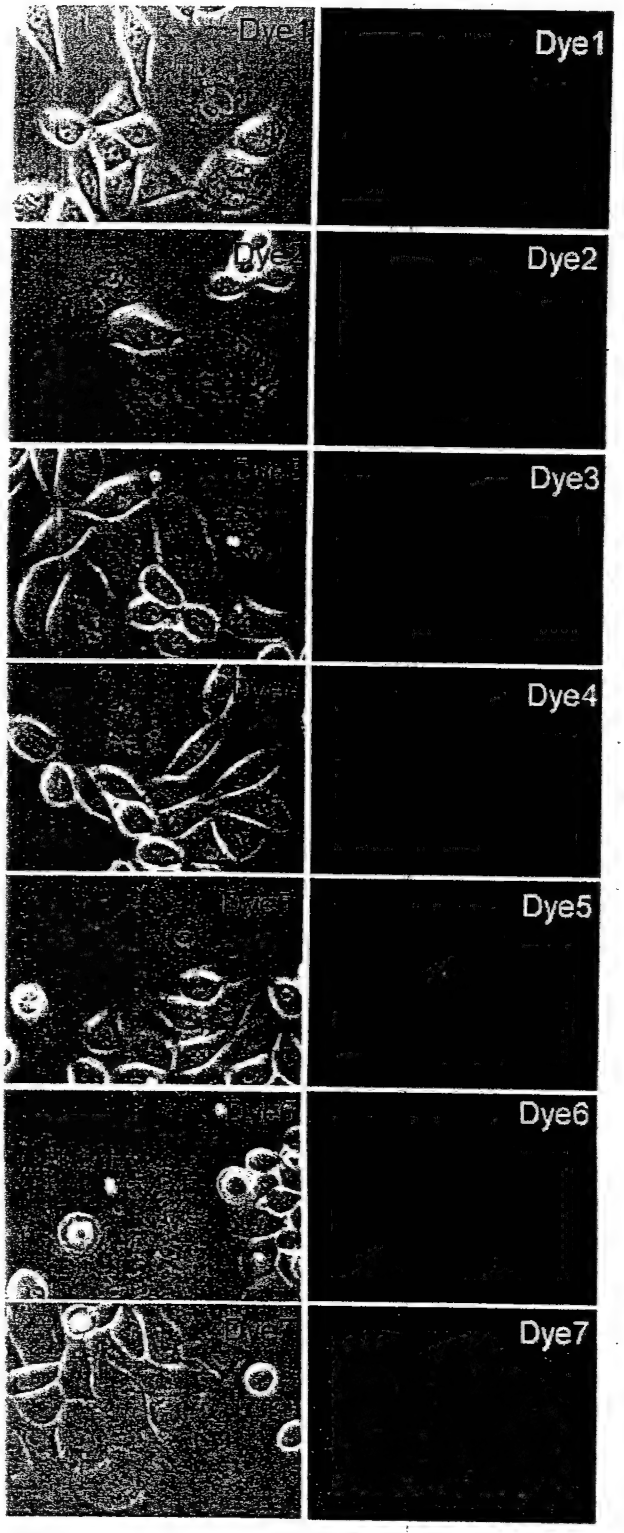

Figure 64: Dye localization in fixed cells. SK-Br-3 cells grown on cover slips were treated for 1 hour with each Dye at 0.5 μM. Cells were washed twice in PBS, and fixed in methanol prior to viewing by epifluorescence microscopy. The left side contains the bright field images while the right side is the corresponding fluorescence image with the Dye indicated on the images. *Imaging system*, SPOT RT. *Camera exposure: Dye 1 and 2, 2 sec; Dye 3, 4 and 5, 500 msec; Dye 6, 7 and 22, 100 msec. Scale bar*, 20 μm.

Figure 64

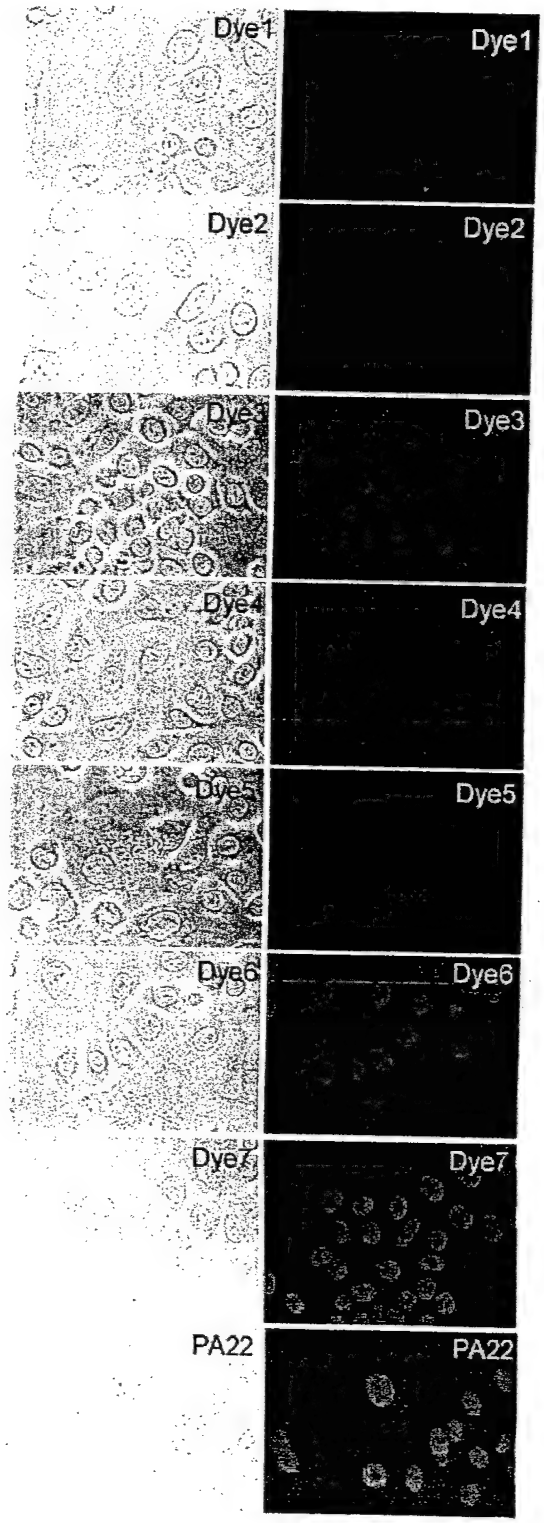
Dye1
Dye1
Dye2
Dye2
Dye3
Dye3
Dye4
Dye4
Dye5
Dye5
Dye6
Dye6
Dye7
Dye7
PA22
PA22

Table 9: Semi-quantitative analysis of each Dye in fixed cells. Semi-quantitative analysis was performed using Image Pro Plus on fixed cell images following treatment with each Dye for 1, 4 and 24 hours. The average images IOD are listed here. *ND*, not determined.

Table 9

	Ave IOD	Ave IOD	Ave IOD
	1hr	4hr	24hr
Dye 1	ND	ND	ND
Dye 2	ND	ND	ND
Dye 3	2	7	43
Dye 4	2	12	30
Dye 5	1	2	8
Dye 6	14	25	107
Dye 7	30	96	394
22	25	31	54

THE JOURNAL OF BIOLOGICAL CHEMISTRY
Vol. 275, No. 32, Issue of August 11, pp. 24246–24254, 2000
Printed in U.S.A.

Targeting the Ets Binding Site of the HER2/*neu* Promoter with Pyrrole-Imidazole Polyamides*

Received for publication, January 31, 2000, and in revised form, May 8, 2000
Published, JBC Papers in Press, May 18, 2000, DOI 10.1074/jbc.M000820200

Shu-Yuan Chiang‡, Roland W. Bürli§¶, Chris C. Benz‖, Loretta Gawron‡, Gary K. Scott‖, Peter B. Dervan¶, and Terry A. Beerman‡§§**

From the ‡Department of Pharmacology and Therapeutics, Roswell Park Cancer Institute, Buffalo, New York 14263, ¶Division of Chemistry and Chemical Engineering and Beckman Institute, California Institute of Technology, Pasadena, California 91125, and the ‖Department of Medicine, University of California, San Francisco, San Francisco, California 94143

Three DNA binding polyamides (1–3) were synthesized that bind with high affinity ($K_a = 8.7 \cdot 10^9$ M^{-1} to $1.4 \cdot 10^{10}$ M^{-1}) to two 7-base pair sequences overlapping the Ets DNA binding site (EBS; GAGGAA) within the regulatory region of the HER2/*neu* proximal promoter. As measured by electrophoretic mobility shift assay, polyamides binding to flanking elements upstream (1) or downstream (2 and 3) of the EBS were one to two orders of magnitude more effective than the natural product distamycin at inhibiting formation of complexes between the purified EBS protein, epithelial restricted with serine box (ESX), and the HER2/*neu* promoter probe. One polyamide, 2, completely blocked Ets-DNA complex formation at 10 nM ligand concentration, whereas formation of activator protein-2-DNA complexes was unaffected at the activator protein-2 binding site immediately upstream of the HER2/*neu* EBS, even at 100 nM ligand concentration. At equilibrium, polyamide 1 was equally effective at inhibiting Ets/DNA binding when added before or after *in vitro* formation of protein-promoter complexes, demonstrating its utility to disrupt endogenous Ets-mediated HER2/*neu* preinitiation complexes. Polyamide 2, the most potent inhibitor of Ets-DNA complex formation by electrophoretic mobility shift assay, was also the most effective inhibitor of HER2/*neu* promoter-driven transcription measured in a cell-free system using nuclear extract from an ESX- and HER2/*neu*-overexpressing human breast cancer cell line, SKBR-3.

Abnormal regulation of gene expression plays an important role in cancer (1, 2). The first step in the regulation of gene expression requires transcription factor (TF)[1] binding to its cognate DNA response element in the gene promoter region (3–5). The ability to preferentially block gene expression by interfering with TF-DNA complexes could be a powerful tool for elucidating how aberrant gene expression contributes to neoplastic phenotypes.

One strategy for developing gene-specific transcriptional inhibitors is to target DNA binding ligands to the cognate DNA response element of a crucial, promoter-regulating TF (6–8). A number of DNA binding natural products and their analogs, which interfere with the binding of TFs to their promoter response elements, are potent inhibitors of gene expression (9–14). Mithramycin, a G,C-specific DNA minor groove binder, inhibits c-Myc expression driven by its G,C-rich P1 promoter (9, 10). Similarly, small molecules such as the DNA intercalator mitoxantrone and the minor groove binding distamycin (Dist), both of which can inhibit the binding of E2F1 to the dihydrofolate reductase promoter, are strong inhibitors of dihydrofolate reductase gene expression (11). However, most DNA binding ligands are not promoter- or TF-specific inhibitors; Dist, for example, is also known to inhibit gene transcription by interfering with the association of TATA box-binding protein to its A,T-rich response element (TATA box) found in the proximal promoter of many genes (12).

We have been investigating a new class of DNA minor groove binding ligands, hairpin pyrrole-imidazole polyamides, as potential promoter- and TF-specific inhibitors of gene expression. In this study we have designed several new polyamides specifically targeted to the Ets binding site (EBS) within the proximal promoter of the HER2/*neu* oncogene. Hairpin polyamides represent a significant advancement in ligand design in that they can achieve a remarkable degree of sequence specificity and high affinity for predetermined DNA sequences (13–15). Polyamides that contain the aromatic rings *N*-methylimidazole (Im) and *N*-methylpyrrole (Py) bind as pairs in an antiparallel fashion to specifically distinguish G·C (Im/Py) from C·G (Py/Im). Py/Py pairs are partially degenerate and bind both A·T and T·A pairs. More than five aromatic rings are overwound relative to the DNA helix, and a β-alanine unit has proven to be a conformationally flexible analog of a pyrrole carboxamide unit (15). A β/β pair can replace a Py/Py pair and allow for recognition of longer sequences while maintaining the specificity for AT/TA base pairs (15). Recently, polyamides designed to interfere with TFIIIA binding to its promoter-response ele-

* This study was supported in part by NCI, National Institutes of Health Grant CA16056 (to T. A. B.), National Institutes of Health Grant GM51747 (to P. B. D.) American Cancer Society Grant DHP 158 (to T. A. B.), and United States Army Medical Research Grants BC960313 (to S. Y. C.), CA36773, and CA44768 (to C. C. B.). The costs of publication of this article were defrayed in part by the payment of page charges. This article must therefore be hereby marked "*advertisement*" in accordance with 18 U.S.C. Section 1734 solely to indicate this fact.

§ Recipient of Swiss National Foundation and the "Novartis Stiftung, vormals Ciba-Geigy-Jubiläums-Stiftung" fellowships.

** To whom correspondence may be addressed: Div. of Chemistry and Chemical Engineering and Beckman Institute, California Institute of Technology, Pasadena, CA 91125. Tel.: 626-395-6002; Fax: 626-683-8753; E-mail: dervan@cco.caltech.edu.

§§ To whom correspondence may be addressed: Dept. of Pharmacology and Therapeutics, Roswell Park Cancer Institute, Elm and Carlton Streets, Buffalo, NY 14263. Tel.: 716-845-3443; Fax: 716-845-8857; E-mail: terry.beerman@roswellpark.org.

[1] The abbreviations used are: TF, transcription factor; Dist, distamycin; EBS, Ets binding site; Im, *N*-methylimidazole; Py, *N*-methylpyrrole; bp, base pair(s); AP, activator protein; EMSA, electrophoretic mobility shift assay; ESX, epithelial restricted with serine box.

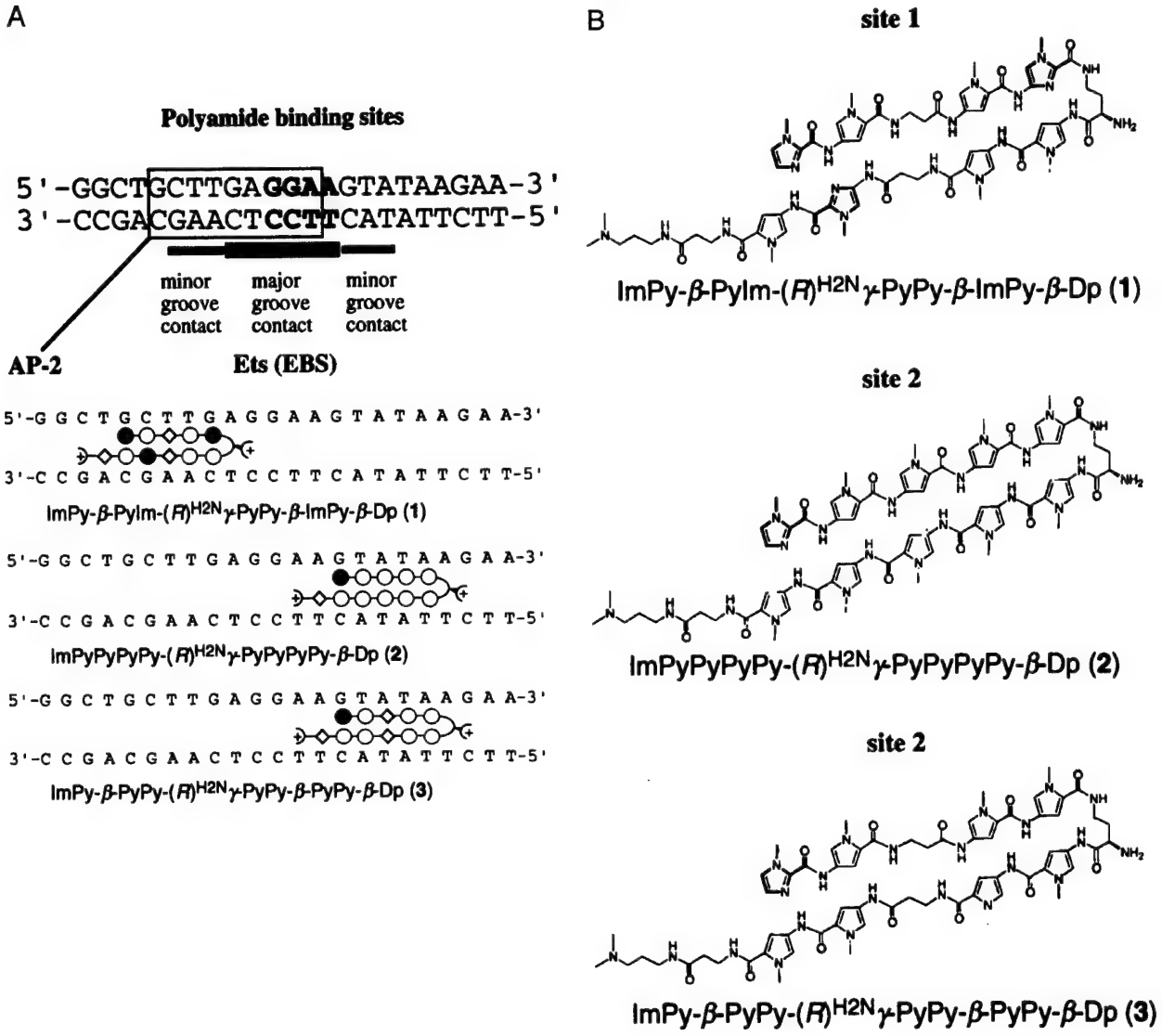

FIG. 1. *A*, HER2/*neu* promoter sequence (and TA5 probe) containing Ets (EBS), AP-2, and TATA box-binding protein-response elements, and showing the 7-bp polyamide binding elements overlapping and positioned just upstream (for polyamide **1**) and downstream (for polyamides **2** and **3**) of the GAGGAA EBS. Schematic binding model of the polyamides; imidazole and pyrrole rings are represented as *shaded* and *unshaded spheres*, respectively, whereas the β-alanine residues are represented as *unshaded diamonds*. *B*, structure of polyamides ImPy-β-PyIm-$(R)^{H2N}$γ-PyPy-β-ImPy-β-Dp (**1**), ImPyPyPyPy-$(R)^{H2N}$γ-PyPyPyPy-β-Dp (**2**), and ImPy-β-PyPy-$(R)^{H2N}$γ-PyPy-β-PyPy-β-Dp (**3**).

ment, were shown to be potent and specific inhibitors of 5 S RNA gene transcription (16, 17). Such designed polyamides have also been shown to specifically inhibit the replication of human immunodeficiency virus, type I virus within the genome of human blood cells (18).

The HER2/*neu* oncogene is amplified and transcriptionally up-regulated in 25–30% of human breast cancers (19). The dramatic loss of ErbB2/HER2 promoter activity in overexpressing (MDA-453) and normal expressing (MCF-7) cells when a mutation of the ErbB2/HER2 promoter's EBS is introduced (GAGGAA to GAGAGA) into a transfected ErbB2 promoter-chloramphenicol acetyltransferase reporter construct demonstrates that the transcriptional up-regulation of HER2/*neu* depends on a highly conserved EBS and its GAGGAA core recognition sequence within the key regulatory region of the HER2/*neu* proximal promoter (20). Recent studies have confirmed, both *in vitro* and *in vivo*, that ErbB2-mediated tumorigenesis could be inhibited by transfecting an Ets repressor that binds specifically and uniquely to the same ErbB2/HER2 promoter's EBS being targeted by our polyamide ligands (21). A number of polyamides were designed to target the EBS and adjacent upstream or downstream flanking sequences unique to this promoter. Three different hairpin polyamides ImPy-β-PyIm-$(R)^{H2N}$γ-PyPy-β-ImPy-β-Dp (**1**), ImPyPyPyPy-$(R)^{H2N}$γ-PyPyPyPy-β-Dp (**2**), and ImPy-β-PyPy-$(R)^{H2N}$γ-PyPy-β-PyPy-β-Dp (**3**) were synthesized to target either the upstream or downstream EBS flanking sequences 5′-TGCTTGA-3′ or 5′-AGTATAA-3′, respectively (Fig. 1*A*). Quantitative footprint titration analysis confirmed their high affinity binding and sequence specificity for the HER2/*neu* EBS. Comparisons were made between these polyamides and the classical three ring DNA minor groove binder, Dist, in their abilities to inhibit binding to the HER2/*neu* EBS by the mammary gland Ets factor, ESX, thought to endogenously regulate this promoter in HER2/*neu* overexpressing human breast cancers (26). Lastly, a cell-free transcription assay was used to evaluate the specific and differential ability of these three polyamides to interfere with HER2/*neu* promoter-driven transcription.

MATERIALS AND METHODS

Synthesis of the Polyamides—The polyamides ImPy-β-PyIm-$(R)^{H2N}$γ-PyPy-β-ImPy-β-Dp (**1**), ImPyPyPyPy-$(R)^{H2N}$γ-PyPyPyPy-β-Dp (**2**), and

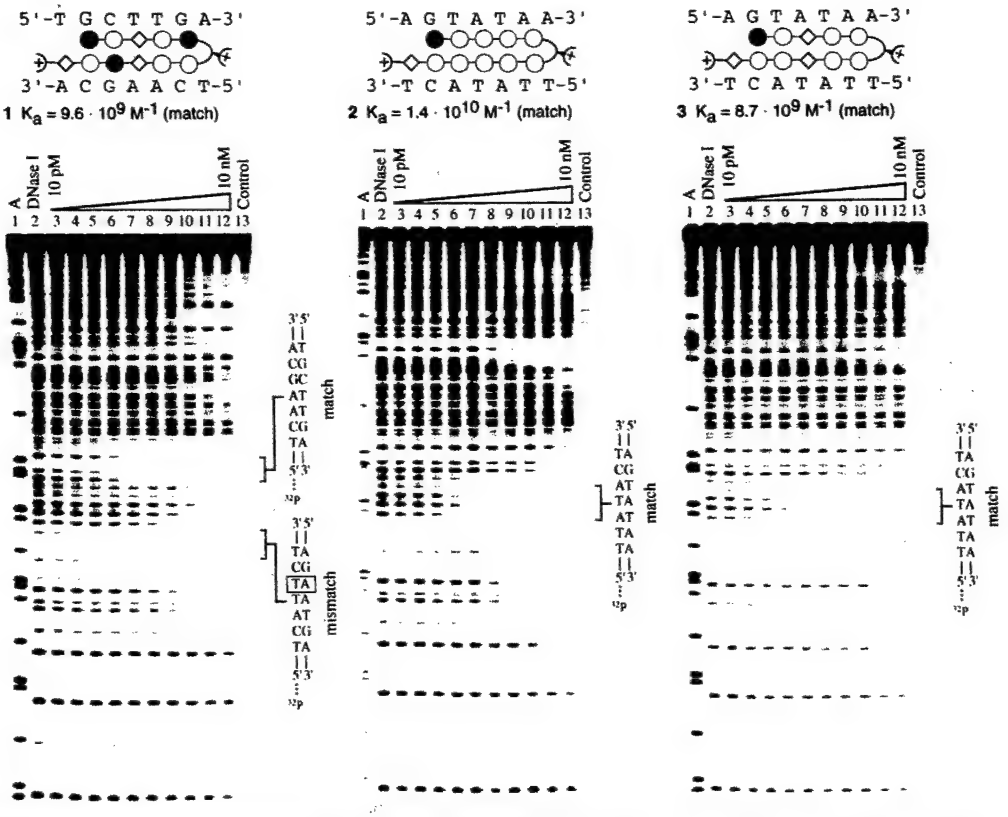

FIG. 2. **Quantitative DNase I footprint titration experiment with the polyamides 1, 2, and 3 on a 5′-^{32}P-radiolabeled, 188-base pair DNA fragment obtained by polymerase chain reaction from the plasmid RO6.** *Lane 1*, A reaction; *lane 2*, DNase I standard; *lanes 3–12*, 10 pM, 20 pM, 50 pM, 100 pM, 200 pM, 500 pM, 1 nM, 2 nM, 5 nM, and 10 nM polyamide; *lane 13*, intact DNA. All reactions contain a 17-kcpm DNA fragment, 10 mM Tris·HCl (pH 7.0), 10 mM KCl, 10 mM $MgCl_2$, and 5 mM $CaCl_2$.

ImPy-β-PyPy-(*R*)^{H2N}γ-PyPy-β-PyPy-β-Dp (**3**) were synthesized from β-alanine-PAM resin using solid phase as described (22) and was characterized by a combination of analytical high pressure liquid chromatography, UV spectroscopy, and matrix-assisted laser desorption ionization/time of flight mass spectroscopy. MS, $^m/_z$ observed for **1,** 1380.7; 1380.7 calculated for $[M + H]^+$; $^m/_z$ observed for **2,** 1480.6, 1480.7 calculated for $[M + H]^+$; $^m/_z$ observed for **3,** 1378.6, 1378.7 calculated for $[M + H]^+$. UV in M^{-1} cm^{-1}, for **1,** 42,500 (ϵ_{242}), 53′100 (ϵ_{298}); for **2,** 58,300 (ϵ_{246}), 79′600 (ϵ_{316}); for **3,** 50,000 (ϵ_{240}), 53′600 (ϵ_{298}).

Quantitative DNase I Footprint Titrations—A 188-base pair (bp) DNA fragment was obtained by polymerase chain reaction using the plasmid RO6 as a template and the primers P1 (5′-GAGAAAGT-GAAGCTGGGAGTT-3′) and P2 (5′-CCTGGTTTCTCCGGTCCCAAT-3′). The primer P2 was 5′-radiolabeled with [γ-^{32}P]ATP using T4-polynucleotide kinase (Roche Molecular Biochemicals). Polymerase chain reaction amplification in the presence of P1, P2 (labeled), plasmid RO6, and *Taq* polymerase (Roche Molecular Biochemicals) gave a 188-bp DNA fragment that was purified on a 6% nondenaturating polyacrylamide gel. All DNase I footprint reactions were performed in a total volume of 400 μl containing a 5′-^{32}P-radiolabeled DNA fragment (17,000 cpm) and final concentrations of 10 mM Tris·HCl, 10 mM KCl, 10 mM $MgCl_2$, 5 mM $CaCl_2$, pH 7.0, and either 0.1–10 nM polyamide or no polyamide (control lanes) (23). The solutions were allowed to equilibrate for 12–14 h at 22 °C. The footprinting reactions were initiated by the addition of 10 μl of a stock solution of DNase I containing 1 mM dithiothreitol and incubated for 7 min at 22 °C. The reactions were stopped by adding 50 μl of a solution of 2.25 M NaCl, 150 mM EDTA, 28 mM base pair calf thymus DNA, and 0.6 mg/ml glycogen and ethanol precipitation. The precipitates were resuspended in 1× Tris borate-EDTA, 80% formamide loading buffer, denaturated by heating at 85 °C for 10 min, and cooled on ice. The reaction products were separated by electrophoresis on a 6% polyacrylamide gel in 1× Tris borate-EDTA at 2000 V for 1 h. Gels were dried on a slab dryer and exposed to a photostimulatable storage phosphorimaging plate (Kodak Storage Phosphor Screen SO230 obtained from Molecular Dynamics) in the dark at 22 °C for 12–24 h. The data from the storage screens were obtained using a Molecular Dynamics 400S PhosphorImager and analyzed by volume integration of the target sites and reference blocks using the ImageQuant version 3.3. software. Equilibrium association constants were determined as described previously (24). Each compound was tested three times; the values for the equilibrium association constants (K_a) correspond to average values from three independent gels.

Cell Culture and Nuclear Extract Preparation—SKBR-3 cells were purchased from ATCC (Rockville, MD) and maintained at 37 °C with 5% CO_2 and in McCoy's 5a medium (Life Technologies, Inc.) with 10% fetal bovine serum. SKBR-3 cells grown to subconfluence were rinsed twice with phosphate-buffered saline, scraped, and collected by centrifugation at 1200 rpm for 5 min, 4 °C (Sorvall RT6000, Newtown, CT). The following steps were performed at 4 °C. Cell pellets were suspended in five times the packed cell volume in buffer A (containing 10 mM Hepes-KOH, pH 7.9, 10 mM KCl, 0.1 mM EDTA, 0.1 mM EGTA, 0.75 mM spermidine, 0.15 mM spermine, and 1 mM dithiothreitol), followed by centrifugation at 1200 rpm for 5 min. The pellet was then resuspended in five times the pellet volume in buffer A, kept on ice for 8 min, and homogenized with 10 strokes using a Dounce homogenizer (tight pestle). The homogenate (~95% lysed cells) was centrifuged at 15,000 rpm for ~1 min, (JA-17 rotor, JA-21 centrifuge; Beckman, Palo Alto, CA). The pellet was resuspended in buffer B with 20 mM Hepes-KOH (pH 7.9), 20% glycerol, 0.2 mM EDTA, 2.0 mM EGTA, 0.75 mM spermidine, 0.15 mM spermine, 2 mM dithiothreitol, and 1 mM phenylmethylsulfonyl fluoride followed by drop addition of an equal volume of buffer B that included 0.75 M NaCl. After rocking for 20 min, the supernatant was collected by centrifugation at 47,500 rpm for 45 min (SW-55 rotor, Beckman), and dialyzed against >100-fold buffer C (20 mM Hepes-KOH, pH 7.9, 20% glycerol, 100 mM KCl, 0.2 mM EDTA, 0.2 mM EGTA, 12.5 mM $MgCl_2$, 2 mM dithiothreitol, and 1 mM phenylmethylsulfonyl fluoride) for 3 h. Precipitated debris was removed by centrifugation at 15,000 rpm (JA-21 centrifuge, JA-17 rotor, Beckman), and the protein content of the nuclear extract was quantitated using the Bio-Rad protein assay.

Proteins, Antibodies, and Oligonucleotides—Recombinant ESX protein was prepared as described (25). Briefly, full-length ESX cDNA was cloned into a pRSET His tag expression plasmid (*Nhe*I-*Hin*dIII; Invitrogen) and expressed in isopropyl-1-thio-β-D-galactopyranoside-induced BL21[DE3] pLysS competent bacteria (Stratagene, La Jolla, CA). His-

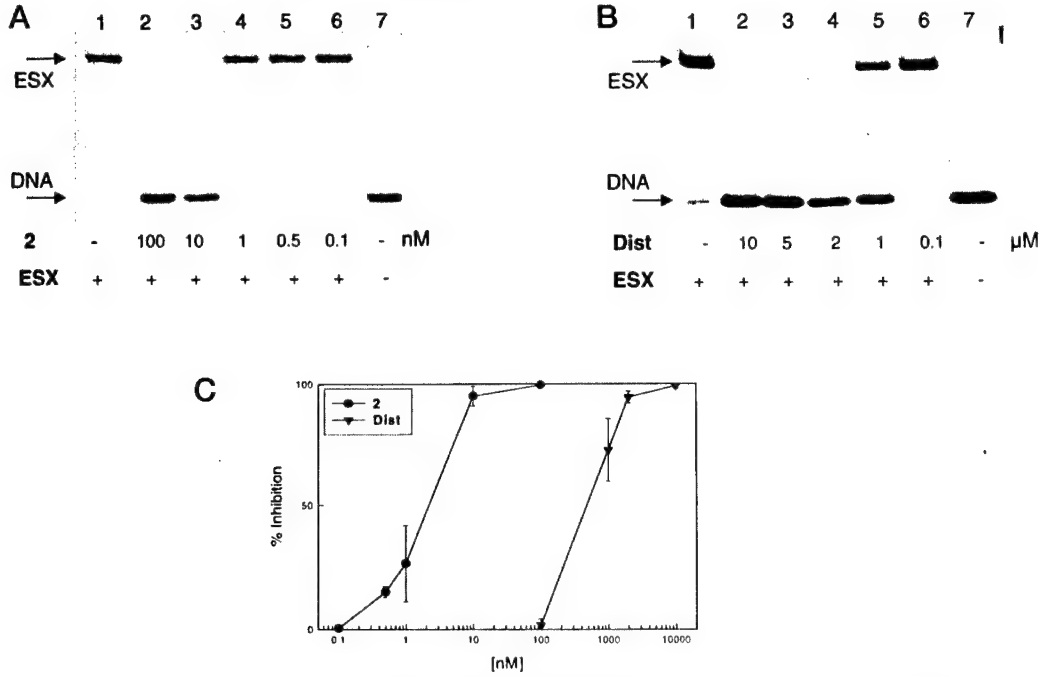

FIG. 3. **EMSA comparison of polyamide 2 *versus* Dist inhibition of ESX-TA5 complex formation.** *A*, EMSA performed in the presence of **2** was used to evaluate the ability of polyamides to inhibit ESX binding to the labeled TA5 HER2/*neu* promoter probe. As described under "Materials and Methods," labeled TA5 probe and compound were incubated for 30 min at room temperature followed by the addition of ESX and subsequent a 30-min incubation. Complexes formed in solution were then separated on a 5% native polyacrylamide gel and visualized by autoradiography. *Lane 1*, control of ESX-TA5; *lanes 2–6*, samples in the presence of **2** at concentrations of 100, 10, 1, 0.5, and 0.1 nM, respectively; *lane 7*, control of free TA5 probe. *B*, EMSA performed in the presence of Dist under the same assay conditions as described for **2**. *Lane 1*, control of ESX-TA5; *lanes 2–6*, samples in the presence of Dist at indicated concentration of 10, 5, 2, 1, and 0.1 μM, respectively; *lane 7*, control of free probe. *C*, inhibition of ESX-TA5 complex formation in the presence of **2** or Dist, plotted as the percentage of control ESX-TA5 complex formation. **2** (●) and Dist (▼) at the indicated concentrations were incubated with the TA5 probe prior to the addition of recombinant ESX protein. The densitometry quantitated data represent the mean values (± S.D.) from at least three separate experiments.

TABLE I
Effects on TF-DNA complex formation by polyamides

Polyamide	TF	IC_{50}	IC_{50} *r* value[a]
		nM	
1	ESX	5	0.16
	AP-2	48	1.55
2	ESX	2.2	0.07
	AP-2	>100	nd[b]
3	ESX	18	0.58
	AP-2	nd	nd
Dist	ESX	500	16.1
	AP-2	6000	193.5

[a] *r* value, the molar ratio of compound to DNA base pairs.
[b] nd, not determined.

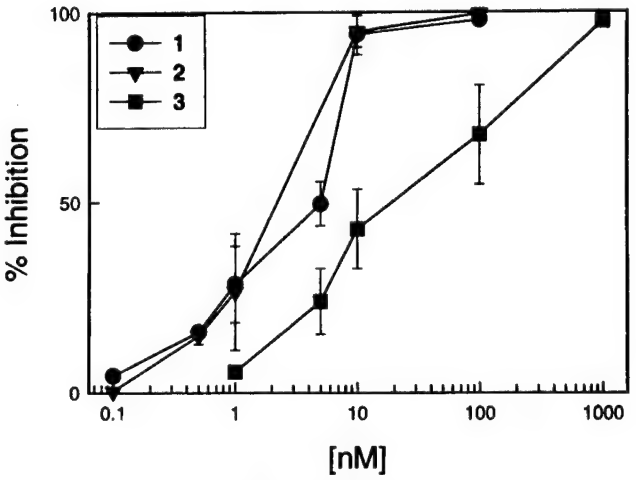

FIG. 4. **Inhibition of ESX-TA5 complex formation after pretreatment of HER2/*neu* promoter probe with various polyamides.** EMSA experiments were performed as described in Fig. 3*A*. Radiolabeled TA5 probe and polyamides **1** (●), **2** (▼), or **3** (■) were incubated for 30 min at room temperature before the addition of recombinant ESX protein. Following gel separation, autoradiography, and densitometry, data are represented as mean values (± S.D.) from three separate experiments.

tagged ESX protein was purified by Ni^{2+}-chelate affinity chromatography, as recommended by the manufacturer (Qiagen Inc., Valencia, CA). Recombinant AP-2 protein was purchased from Promega Co. (Madison, WI). Monoclonal antibody against AP-2 was purchased from Santa Cruz Biochemical (Carpenteria, CA), and the anti-ESX affinity-purified rabbit polyclonal was prepared as described previously (26). A 34-mer DNA oligonucleotide (oligo) containing the EBS and derived from the HER2/*neu* proximal promoter (TA5 sequence shown in Fig. 1*A*) and its complementary strand, were synthesized by the Biopolymers facility (Roswell Park Cancer Institute, Buffalo, NY). Oligos were gel-purified, annealed, and 5′-end-labeled with [γ-^{32}P]ATP using T4-polynucleotide kinase (New England BioLabs, Beverly, MA) as described previously (27).

Mobility Shift Assay—Demonstration of TFs binding to their DNA response elements in the proximal HER2/*neu* promoter was performed by EMSA using recombinant TFs (ESX, AP-2), duplexed and 5′-end-labeled TA5 promoter probe, with/without anti-TF antibody. In general, recombinant protein at the indicated concentrations and 1 nM ^{32}P-labeled DNA probe were incubated in a reaction buffer containing 25 mM Tris (pH 7.5), 30 mM KCl, 5% glycerol, 0.1% Nonidet P-40, bovine serum albumin (100 μg/ml), and 1 mM dithiothreitol. After incubation at room temperature for 30 min, samples were loaded onto 5% native polyacrylamide gels running with Tris borate-EDTA buffer (44.5 mM Tris base, 44.5 mM boric acid, 1 mM EDTA, pH 8.3). The dried gel was exposed to Kodak film and the protein-DNA complexes were quantitated by computing laser densitometry (Molecular Dynamics, Sunnyvale, CA).

Identification of specific protein-DNA complexes was confirmed by the addition of specific antibodies in the EMSA reaction conditions, as indicated. The ability of polyamides to interfere with the formation of a protein-DNA complex was determined by EMSA. For polyamide effects

on monomeric ESX binding to TA5 (ESX-TA5 complex formation), assays were performed in two ways: (i) polyamides were incubated with a ^{32}P-labeled probe at room temperature for 30 min prior to the addition of ESX protein, and (ii) ESX protein was complexed with the probe prior to polyamide treatment. The inhibition of ESX-TA5 complex formation was measured by comparing polyamide-treated with nontreated samples. Polyamide ability to inhibit dimeric AP-2 binding to TA5 (AP-2-TA5 complex formation) was measured in a similar manner. IC_{50} values (concentration of compound required for 50% inhibition of protein-DNA complex formation) were determined to express the inhibitory activity of each agent; these IC_{50} polyamide concentrations were also expressed as *r* values, the molar ratio of ligand to DNA base pairs.

Cell-free Transcription Assay—In vitro transcription was performed in a cell-free system composed of DNA template, SKBR-3 nuclear extract, and buffer containing 12 mM Hepes-KOH (pH 7.9), 60 mM KCl, 7.5 mM $MgCl_2$, 12% glycerol, 0.12 mM EDTA, 0.12 mM EGTA, 1.2 mM dithiothreitol, and 0.6 mM phenylmethylsulfonyl fluoride. The transcription DNA template consisted of CsCl-purified plasmid DNA containing the ~500-bp RO6 HER2/*neu* promoter fragment (20), inserted into a pCDNA3-Luc expression vector (Invitrogen, Carlsbad, CA), and linearized by restriction with *Sph*I (New England BioLabs, Beverly, MA). Into a 25-μl reaction of SKBR-3 nuclear extract was added 1 μg of *Sph*I-digested DNA, nuclear extracts, 0.5 μl of each nucleotide (20 mM of ATP, GTP, UTP, and 100 μM CTP), 10 μCi of [α-^{32}P]CTP (800 Ci/mmole; NEN Life Science Products), 1 μl of RNAsin (40 units/μl; Roche Molecular Biochemicals), and 1.4 μl of EDTA (2.5 mM). Transcript formation proceeded with incubation at 30 °C for 60 min, and the reaction was stopped by adding 325 μl of 10 mM Tris base (pH 8.0), 7 M urea, 350 mM NaCl, 1% SDS, and 100 μg of tRNA, followed by phenol-chloroform-isoamyl alcohol extraction and ethanol precipitation. Samples were resuspended in formamide-loading dye and heated at 90–95 °C for ≥1 min before loading onto a 4%, 7 M urea-polyacrylamide gel. The ^{32}P signal from a dried gel was visualized using a PhosphorImager screen and quantitated by computing laser densitometry (Molecular Dynamics, Sunnyvale, CA).

As with EMSA assessment of polyamide activity, ligand ability to inhibit transcript formation driven off the HER2/*neu* promoter was analyzed in two ways: (i) DNA template was incubated with polyamide at the indicated concentration in a total volume of 10 μl for 30 min prior to the addition of nuclear extract and radiolabeled nucleotide pool, and (ii) preincubation of nuclear extract and DNA template for 15 min was followed by the addition of ligand for another 30 min in the total reaction volume to which radiolabeled nucleotide pool was then added. The degree of transcription was measured by quantitating transcript formation in ligand-treated *versus* untreated (control) samples and calculating IC_{50} and *r* values. T3 transcript (250 bases; Promega Co., Madison, WI) was used as an internal control. In addition, a time course assay was used to compare transcriptional inhibition off the HER2/*neu* promoter in the presence of Dist *versus* polyamide **2** using our previously described procedure (11). For these time course assays, following the addition of ligands and nucleotides to the premixed template and nuclear extract volume, the reaction was stopped at different time points (0–60 min), and the newly formed transcripts were quantitated as described above.

RESULTS

Design of HER2/neu Promoter Binding Polyamides—We used the simple pairing code (15) to design polyamides that bind the 5′- and 3′-flanking sequences overlapping the EBS (GAGGAA) within the endogenous HER2/*neu* proximal promoter, the RO6 HER2/*neu* promoter-driven transcript template, and the EMSA TA5 probe. The proximal HER2/*neu* promoter sequence containing this EBS is shown in Fig. 1*A*, and this HER2/*neu* EBS has previously been shown to bind with high affinity to the potent and epithelial-restricted Ets transactivator, ESX (25, 26). All Ets family members bind to the major groove of DNA and have additional critical phosphate contacts along flanking minor groove sequences (28, 29). Whereas the GGAA core of the EBS is the same for virtually all Ets proteins, these 5′- and 3′-sequences immediately adjacent to the EBS core are often promoter- and Ets factor-specific. Thus, we synthesized three polyamides to target 7 bp of the HER2/*neu* promoter sequence 5′ and 3′ of the EBS core; polyamide **1** was designed to bind immediately upstream of the ESX core binding site at 5′-TGCTTGA-3′ (site 1), whereas

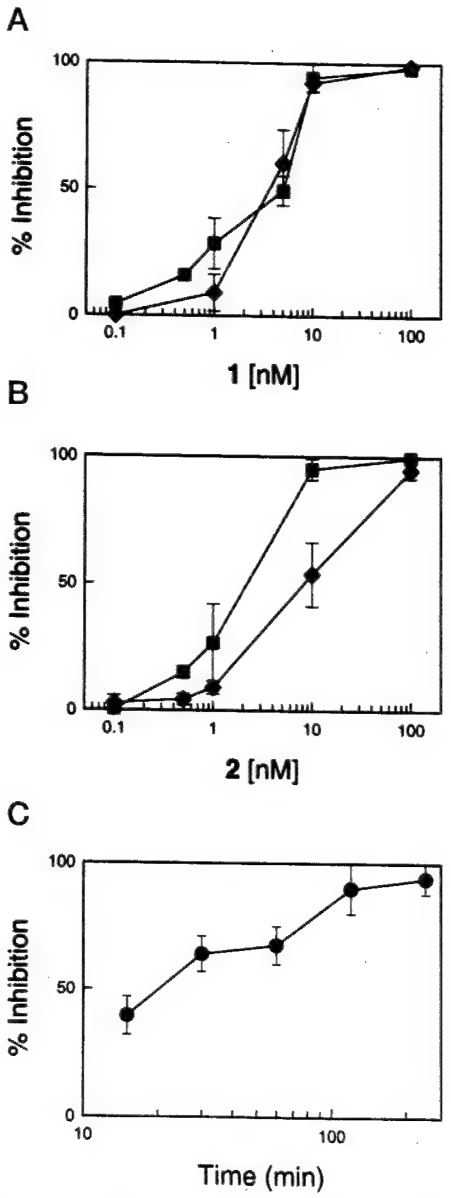

FIG. 5. **Comparative HER2/*neu* inhibitory effects of polyamides administered before or after formation of ESX-TA5 complexes.** EMSA performed when **1** (*A*) or **2** (*B*) were added at indicated concentrations either before (■) or after (♦) formation of ESX-TA5 complexes. Following gel separation, autoradiography, and densitometry, data are represented as mean values (± S.D.) from at least three separate experiments. A time course assay was used to estimate the time required for **2** to reach steady-state equilibrium in terms of inhibition of ESX-TA5 complex formation (*C*). ESX and radiolabeled TA5 probe were incubated at room temperature for 30 min followed by the addition of polyamide **2** at 10 mM for 240, 120, 60, 30, or 15 min; replicate assay results are expressed as mean values (± S.D.).

polyamides **2** and **3** were designed to bind immediately downstream and across the adjacent TATA box at 5′-AGTATAA-3′ (site 2).

Selectivity and High Affinity Binding of Polyamides to the HER2/neu Promoter EBS—Quantitative DNase I footprint titration analysis showed that polyamides **1, 2,** and **3** bind with high affinity to their target sites (Fig. 2). Polyamide **1** binds with an equilibrium association constant $K_a = 9.6 \cdot 10^9\ M^{-1}$ to its match site (5′-TGCTTGA-3′). It binds by a factor of ~2 less strongly to a single base pair mismatch site (5′-AGAATGA-3′) located downstream with respect to the ESX binding site ($K_a = 4.5 \cdot 10^9\ M^{-1}$). Polyamides **2** and **3** both bind with high affinity

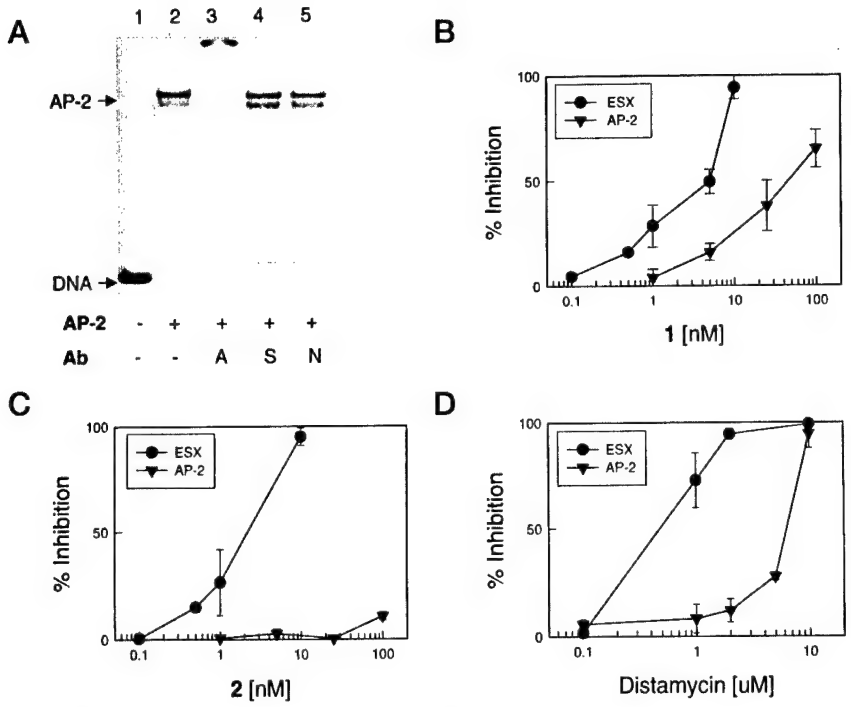

FIG. 6. **Antibody-specific AP-2 binding to the HER2/*neu* promoter probe TA5, and polyamide *versus* Dist inhibition of AP-2-TA5 complex formation.** Demonstration of specific AP-2 binding to TA5 confirmed by AP-2 antibody-induced supershifting on EMSA. Recombinant AP-2 protein with/without monoclonal antibodies were incubated for 10 min prior to the addition of radiolabeled TA5 probe, as described under "Materials and Methods." *A, lane 1*, control of free TA5 probe; *lane 2*, AP-2-TA5 complexes; *lanes 3–5*, reactions with antibodies of *A* (AP-2), *S* (Sp1), and *N* (normal immunoglobulins), showing formation of a slower migrating (supershifted) TA5 complex only in the presence of AP-2-TA5 binding monoclonal. Inhibition of the AP-2-TA5 complexes (▼) was compared with EMSA formation of ESX-TA5 complexes (●) in the presence of (*B*) **1**, (*C*) **2**, or (*D*) Dist. All results are expressed as mean values (± S.D.) from replicate experiments each performed with duplicate samples.

to their target site (5′-AGTATAA-3′, $K_a = 1.4 \cdot 10^{10}$ M^{-1} and $K_a = 8.7 \cdot 10^9$ M^{-1}, respectively).

Polyamide 2 Inhibition of Ets Binding to the HER2/neu Promoter—Because Dist can also bind to the TATA box contained in the 3′-EBS element targeted by two of the polyamides (12), polyamide **2** and Dist were compared by EMSA for their abilities to inhibit ESX binding to the HER2/*neu* promoter probe, TA5. Incubation of **2** with TA5 followed by the addition of ESX resulted in a concentration-dependent inhibition of ESX-TA5 complex formation; 10 nM **2** inhibited complex formation up to 95%, whereas as little as 1 nM resulted in a detectable decrease in complex formation (Fig. 3*A*, *lanes 2–4*). The pattern of inhibition of ESX-TA5 complex formation by Dist was similar, but significantly higher Dist concentration was required to achieve the same degree of inhibition observed by **2**, because Dist at 2000 nM diminished complex formation by ~95% (Fig. 3*B*, *lane 4*). Whereas 100 nM of **2** inhibited ESX-TA5 complex formation almost entirely, 100 nM Dist had no effect on ESX-TA5 complex formation (Fig. 3*A*, *lane 2* and Fig. 3*B*, *lane 6*). Quantitation of the data in Fig. 3*C* indicated that 2.2 nM **2** and 500 nM Dist are needed to inhibit complex formation by 50% (IC_{50}); Table I also shows the activity of individual polyamides at inhibiting protein-DNA complex formation expressed as *r* values, the molar ratio of ligand to DNA base pairs.

Inhibitory Effects of Polyamides (1, 2, and 3) on Ets Binding to the HER2/neu Promoter—Because **1** and **2** recognize DNA elements upstream and downstream of the core EBS while **3** also recognizes the same downstream flanking element as **2** (Fig. 1), EMSA was used to test the relative ability of each polyamide to inhibit ESX binding to the HER2/*neu* promoter probe TA5. As shown in Fig. 4, **1** and **2** appeared similar in their ability to inhibit complex formation with respective IC_{50} values of 5 and 2.2 nM. In contrast, **3** required a 9-fold higher concentration (18 nM) to prevent Ets-DNA complex formation by 50% as compared with **2** (Fig. 4 and Table I).

For certain TF/DNA inhibitory drugs, equilibrium conditions demand greater drug concentrations to inhibit preformed DNA-bound complexes as opposed to preventing the initial formation of such complexes (6). For polyamide **1**, however, similar experimental conditions were observed for inhibition of Ets-DNA complexes whether ligand was added before or after ESX binding to the HER2/*neu* promoter probe, because at 10 nM polyamide **1** concentration nearly the same level of ESX-TA5 complexes were formed within 30 min no matter which order the reagents were added (Fig. 5*A*). In contrast, **2** required 10-fold more ligand to obtain equal inhibition when added after ESX-TA5 complex formation as compared with the addition of **2** before complex formation (Fig. 5*B*). A time course assay using 10 nM of **2** indicated that the percentage of ESX-TA5 complexes inhibited by **2** increased with longer incubation time such that a ≥4 h polyamide **2** incubation was needed to achieve equilibrium conditions and maximal inhibition when **2** was added after the initial formation of ESX-TA5 complexes (Fig. 5*C*).

Inhibitory Effects of Polyamides on AP-2 Versus Ets Binding to the HER2/neu Promoter—Previous studies have suggested that AP-2 contributes to the overexpression of HER2/*neu*, and footprinting analysis has revealed that there are several AP-2 sites in the proximal HER2/*neu* promoter (30). We also had observed that both endogenous and recombinant AP-2 binds to a G-rich sequence just upstream of the EBS on the HER2/*neu* promoter. Dimeric binding of AP-2 to this G-rich element in the TA5 probe (Fig. 1) is demonstrable by EMSA and confirmed by the supershifting effect of an AP-2 monoclonal; in contrast, antibodies nonreactive to AP-2 had no effect on this AP-2-TA5 complex (Fig. 6*A*). Because AP-2 interacts with this G-rich element adjacent to the EBS in TA5, it was of interest to know whether the EBS-targeted polyamides would affect the binding of AP-2 to this HER2/*neu* promoter probe. Fig. 6*B* shows that **1**

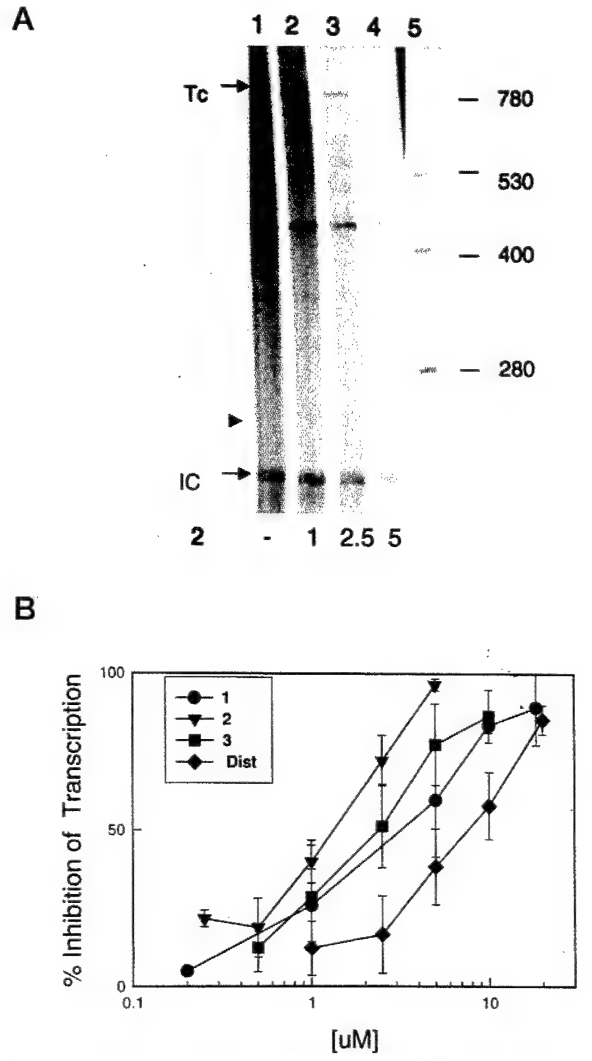

FIG. 7. **Polyamide and Dist pretreatment of the HER2/*neu* promoter inhibits its transcriptional activity.** HER2/*neu* promoter-driven transcription was measured in a cell-free assay as described under "Materials and Methods"; briefly, compound at the indicated concentration was incubated with a *Sph*I-restricted HER2/*neu* promoter-driven transcription template (RO6) at 30 °C for 30 min, followed by the addition of SKBR-3 nuclear extract and a radiolabeled pool of nucleotide precursors. Transcription was allowed to proceed for 60 min at 30 °C with the expected ~760-base transcript identified by gel electrophoretic separation and phosphorimaging of the scanned gel. Scan from a representative experiment performed in the presence of polyamide **2** is shown in *A*. *Lane 1*, untreated control; *lanes 2–4*, cell-free transcription performed in the presence of 1, 2.5, and 5 μM **2**; *lane 5*, RNA marker. *IC*, internal control; *TC*, 760-base transcript. Activities of polyamides, **1** (●), **2** (▼), **3** (■), and Dist (◆) are presented as percentage inhibition of transcript formation comparing the compound-treated condition with untreated control (*B*) and transcript formation in individual samples normalized to the internal control. Results represent the mean values (± S.D.) of replicate experiments.

was capable of inhibiting EMSA-detected AP-2-TA5 complexes in a concentration-dependent manner and with an IC_{50} = 48 nM. In contrast, **2** was unable to block complex formation even at the highest concentration (100 nM) tested (Fig. 6*C*).[2] Likewise, the pattern of inhibition of AP-2-TA5 complexes by Dist was similar to that of **2** in that micromolar concentrations were required to significantly inhibit complex formation (Fig. 6*D* and Table I). All these compounds were more efficient at inhibiting formation of ESX (*versus* AP-2) complexes on the HER2/*neu* promoter probe, with **2** being the most specific and most potent inhibitor.

[2] Polyamide concentration greater than 100 nM caused smearing of the DNA under our assay conditions.

TABLE II
Effects on the in vitro transcription by polyamides

Polyamide	IC_{50}	IC_{50} *r* value
	μM	
1	3.2	0.02
2	1.4	0.009
3	2.4	0.015
Dist	7.4	0.05

Transcription Inhibiting Effects of Polyamides on the HER2/neu Promoter—To determine whether the effects of polyamides on Ets-DNA complex formation resulted in an ability to influence biological function, *in vitro* transcription assays were performed using a HER2/*neu* promoter-driven DNA template. With the ~500 bp of HER2/*neu* promoter-inserted plasmid (RO6) linearized with *Sph*I as DNA template and SKBR-3 nuclear extracts (endogenously enriched in ESX, AP-2, TATA box-binding protein, etc.) to provide the transcriptional machinery, a ~760-base transcript is produced in this cell-free system. Compounds were first incubated with the DNA template prior to the addition of nuclear extracts and radiolabeled pool of nucleotides. A representative gel shown in Fig. 7*A* demonstrates the ability of **2** to block synthesis of the 760-base transcript in a concentration-dependent manner. Compared with the untreated control, 5 μM of **2** inhibited transcript synthesis by 95%; whereas 1 μM produced less than 50% inhibition of transcript formation, at higher polyamide concentrations there was some evidence of the partial transcript production (Fig. 7*A*, *lanes 3* and *4*). Comparative inhibition of HER2/*neu* promoter-driven transcription by **1, 2, 3,** and Dist is shown in Fig. 7*B*. The order of transcription inhibiting potency (**2** > **3** > **1** > Dist) is somewhat different from the EMSA ESX-TA5 complex inhibiting potency for these compounds. Their corresponding IC_{50} values are 1.4 μM for **2,** 2.4 μM for **3,** 3.2 μM for **1,** and 7.4 μM for Dist; their *r* values are also shown in Table II.

Because EMSA results demonstrated differences between the ability of **1** and **2** to inhibit Ets-DNA complexes when ligand was given before or after initial formation of the ESX-TA5 complex (Fig. 5), to determine if the order of addition of polyamides influenced their transcription inhibitory activity, nuclear extracts were allowed to interact with the promoter and DNA template prior to ligand exposure. Polyamide effectiveness appeared to be reduced when tested in this fashion (Fig. 8). For example, concentrations of **2** at 1.4 or 4.2 μM were required to inhibit transcription by 50% when ligand was added before or after nuclear extract binding with the R06 template (Fig. 8*A*). In the case of **1,** a 2-fold higher ligand concentration was needed to inhibit transcription (6.4 μM) when extract was prebound to template (Fig. 8*B*).

Previous time course studies with DNA binding and transcription-inhibiting drugs have shown that the degree of transcription inhibition can change in relation to the *in vitro* reaction time in the presence of moderately inhibiting drug concentrations (11). Conducting similar time course experiments with the most potent inhibitor **2** revealed a plateau level of transcription inhibition at all time points from 10–60 min (Fig. 9). In contrast, the level of transcription inhibition by Dist declined somewhat in relation to incubation time. These time course differences between **2** and Dist might be accounted for by the higher DNA binding affinity of the polyamide, making it less likely that ligand is released from the template and transcription is allowed to resume during the longer exposure times.

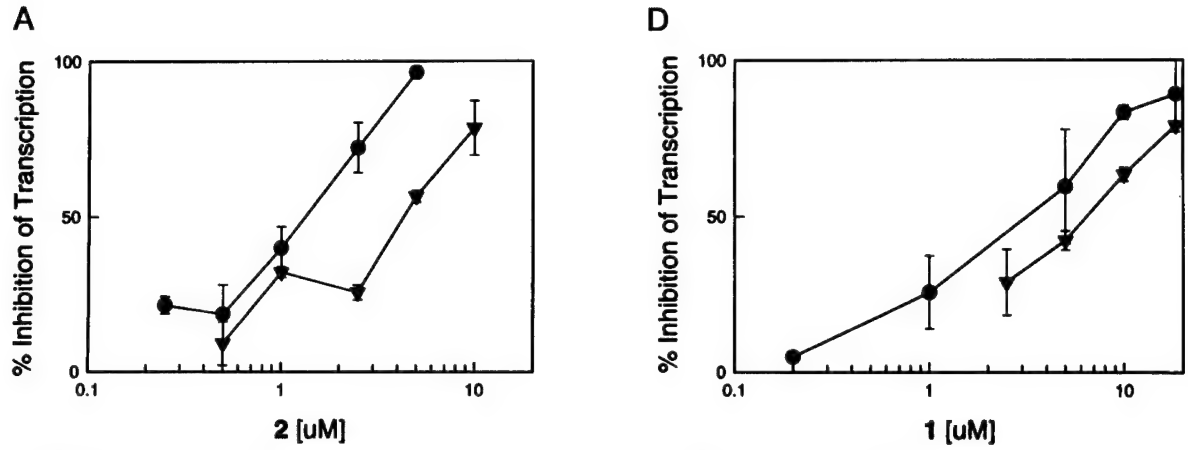

FIG. 8. **Comparative inhibition of HER2/*neu* promoter-driven transcription when polyamides are administered before or after promoter binding to endogenous transcription factors contained in SKBR-3 nuclear extract.** The experimental procedure was similar to that described in Fig. 7*A* except that the promoter-driven DNA template was incubated with SKBR-3 nuclear extracts for 15 min before the addition of a labeled pool of nucleotide precursors and polyamides **2** (*A*) or **1** (*B*). The percent inhibition of transcript formation (▼) produced by the individual ligands was compared with that produced when ligand exposure to template preceded the addition of nuclear extract (●). Results represent the mean (± S.D.) of replicate experiments.

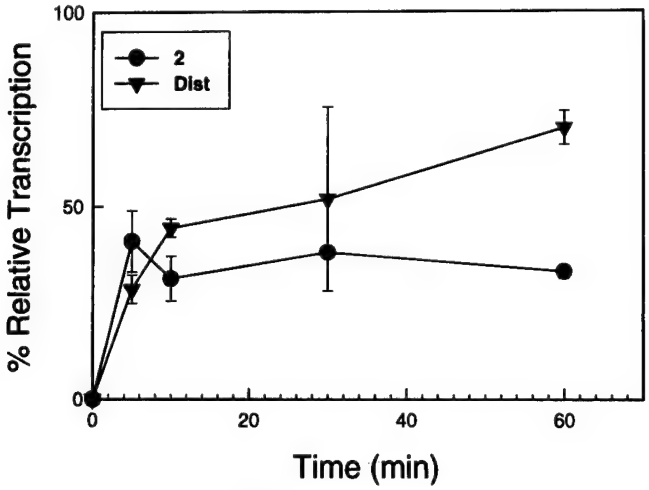

FIG. 9. **Inhibition of HER2/*neu* promoter-driven transcription when compound is administered after template binding to nuclear extract and as a function of exposure time.** The experimental procedure was similar to that described in Fig. 8 except that the cell-free transcription reaction was stopped after a 5-, 10-, 30-, or 60-min exposure to **2** (●) and Dist (▼). Results represent the mean (± S.D.) of replicate experiments.

DISCUSSION

In this study, we examined the ability of sequence-specific polyamides to inhibit Ets-DNA complex formation and EBS-regulated transcription off the HER2/*neu* promoter. Polyamides were synthesized that recognize different elements overlapping and flanking the GAGGAA EBS, located adjacent to and 5′ of the TATA-box in the regulatory portion of the proximal HER2/*neu* promoter (20). As compared with the TATA box binding natural product Dist, three designed sequence-specific polyamides were more effective at inhibiting EBS complex formation with the mammary gland Ets transactivator, ESX, as well as HER2/*neu* driven transcription from a ~500 bp HER2/*neu* promoter sequence known to be regulated at the EBS as well as other endogenous response elements (*e.g.* AP-2, Sp1, CAAT, and TATA boxes). Of the three polyamides, **2** was the most strongly binding and effective HER2/*neu* promoter inhibitor, binding with a $K_a = 1.4 \cdot 10^{10}$ M^{-1} to the 3′-flanking EBS element that includes the promoter's TATA box.

Comparison of the three polyamides (**1**-**3**) with Dist for inhibition of protein-DNA complex formation on the HER2/*neu* promoter probe, TA5, revealed the vastly enhanced potency and specificity of the high affinity hairpins as opposed to the latter natural product. Because both Dist and polyamides **2** and **3** bind the same TATA box containing the 3′-EBS element (Fig. 1), the higher binding affinity of **2** for this element likely contributed to its greater inhibitory activity over both Dist and polyamide **3**. However, because Ets family members also make minor groove phosphate contacts in addition to their major groove base contacts, some of the enhanced inhibitory effects of both these polyamides over Dist may be attributed to steric effects restricting Ets (ESX) access to the HER2/*neu* EBS (28, 31). With a similar comparison in the present study, HER2/*neu* promoter-targeted polyamides were shown to differentially affect ESX and AP-2 binding to adjacent DNA response elements. The binding of polyamide **1** to its 5′-EBS element partially impinges on the G-rich AP-2 binding site present in the TA5 probe (Fig. 1), probably accounting for the observed ~10-fold less effective inhibitory activity of **1** at blocking formation of AP-2-TA5 *versus* ESX-TA5 complexes (Fig. 6*B*). Comparing Dist and polyamide **2** (Fig. 6, *C* and *D*), both of which bind the same 3′-EBS element located more remote from the AP-2 binding element in TA5, demonstrated the vastly improved promoter specificity of a designed polyamide over a less specific natural product like Dist, because the latter showed some AP-2 inhibitory activity whereas the former showed none despite its potent ESX-TA5 inhibitory activity over the same concentration range.

Small molecules that bind DNA near or at a TF response element typically require more time (or higher concentrations) to achieve steady-state inhibition of protein-DNA complexes when added after rather than before the formation of these complexes (6, 12, 27). Differences in this regard were noted between polyamides **1** and **2** when EMSA was carried out with ligands added before or 30 min after formation of ESX-TA5 complexes; polyamide **1** showed no significant impact by delayed administration but **2** showed a near 50% increase in its IC_{50} (Fig. 5, *A* and *B*). However, by increasing its post-treatment incubation time from 30 min to 240 min, a 10 nM dose of polyamide **2** regained its full inhibitory activity as seen with a 30-min pretreatment at this same dose (Fig. 5*C*), demonstrating that **2** required longer post-treatment exposure than **1** to achieve its steady-state inhibitory potential. The difference in

this regard between polyamides **1** and **2** likely reflects 3′-*versus* 5′-asymmetry in the TA5-bound ESX complex, resulting in greater structural interference and reduced access to the TA5 element recognized by **2** in the presence of preformed ESX-TA5 complexes (Fig. 9).

Polyamide **2,** which most effectively inhibited ESX-TA5 complex formation at equilibrium also most effectively inhibited HER2/*neu* promoter-driven transcription, assayed in a cell-free system utilizing endogenous ESX, AP-2, TATA box-binding protein, and other transcriptional components endogenously present in a nuclear extract of the HER2/*neu* overexpressing breast cancer cell line, SKBR-3. Interestingly, polyamide **3,** which was 3-fold less inhibitory than **1** at inhibiting formation of ESX-TA5 complexes on the 34-bp TA5 promoter probe (IC_{50} of 18 nM *versus* 5 nM), was at least as effective as **1** at inhibiting cell-free transcription off the ~500-bp (R06) HER2/*neu* promoter-driven template. Moreover, the inhibitory activity of polyamide **1,** which was unaffected in EMSA by prebinding of ESX to TA5, was moderately reduced in the cell-free transcription assay by prebinding of nuclear extract to the HER2/*neu* promoter-driven template, as was the transcription inhibitory activity of polyamide **2**. Similar discordances were observed in comparisons of mitoxantrone and Dist as inhibitors of both protein-DNA complex formation and cell-free transcription with the DHFR promoter (11). Possible variables accounting for these discordances in the present study include the multiplicity of endogenous HER2/*neu* promoter binding factors present in the nuclear extract fueling the transcription assay (*versus* the single protein component in the EMSA assay) and potentially different numbers of lower affinity binding sites for each polyamide on the linearized R06 plasmid-containing HER2/*neu* promoter-driven template (*versus* the 34-bp TA5 EMSA probe). To address the potential impact of DNA content (bp) as a discordance-inducing variable between the EMSA and cell-free transcription assay, *r* values were calculated to compare the molar ratios of polyamide to DNA content (Tables I, and II). The degree of difference between the EMSA and transcription assay *r* values for Dist is most notable and without obvious explanation. However, the lower overall *r* values among polyamides tested by transcription assay *versus* their EMSA determined values suggest that differences in total DNA content or polyamide binding sites on the HER2/*neu* promoter-containing plasmid template did not substantially contribute to the discordances noted above.

In summary, polyamides designed to selectively target critical 7-bp elements flanking and overlapping on a singular EBS in the regulatory region of the proximal HER2/*neu* promoter were shown to exhibit high affinity binding to their respective elements and to specifically disrupt binding of a HER2/*neu* promoter EBS candidate, ESX. These Ets-DNA complex inhibiting hairpin polyamides were significantly more potent inhibitors of HER2/*neu* promoter-driven transcription than the natural product Dist, a TATA box minor groove binder, and less effective Ets-DNA complex inhibitor. The differences noted in the HER2/*neu* promoter inhibiting activities of these polyamides is thought to be because of both their respective binding affinities and the choice of EBS flanking elements targeted for polyamide binding. These differences may implicate vulnerable promoter elements for future attempts to repress transcription of the overexpressing HER2/*neu* oncogene. Studies are now underway to evaluate the effectiveness of polyamides as HER2/*neu* transcription inhibitors in whole cell systems.

REFERENCES

1. Look, T. A. (1995) *Adv. Cancer Res.* **67,** 25–57
2. Epstein, F. H. (1994) *N. Engl. J. Med.* **330,** 328–336
3. Ellenberger, T. (1994) *Curr. Opin. Struct. Biol.* **4,** 12–21
4. Brennan, R. G. (1993) *Cell* **74,** 773–776
5. Gehring, W. J., Qian, Y. Q., Billeter, M., Furukubo-Tokunaga, K., Schier, A. F., Resendez-Perez, D., Affolter, M., Otting, G., and Wuthrich, K. (1994) *Cell* **78,** 211–223
6. Welch, J. J., Rauscher, F. J., III, and Beerman, T. A. (1994) *J. Biol. Chem.* **269,** 31051–31058
7. Broggini, M., and D'Incalci, M. (1994) *Anticancer Drug Design* **9,** 373–387
8. Sun, D., and Hurley, L. (1995) *Curr. Biol.* **2,** 457–469
9. Snyder, R. C., Ray, R., Blume, S., and Miller, D. M. (1991) *Biochemistry* **30,** 4290–4297
10. Hardenbol, P., and Van Dyke, M. W. (1992) *Biochem. Biophys. Res. Commun.* **185,** 553–558
11. Chiang, S. Y., Azizkhan, J. C., and Beerman, T. A. (1998) *Biochemistry* **37,** 3109–3115
12. Bellorini, M., Moncollin, V., D'Incalci, M., Mongelli, N., and Mantovani, R. (1995) *Nucleic Acids Res.* **23,** 1657–1663
13. Geierstanger, B. H., Mrksich, M., Dervan, P. B., and Wemmer, D. E. (1994) *Science* **266,** 646–650
14. Swalley, S. E., Baird, E. E., and Dervan, P. B. (1996) *J. Am. Chem. Soc.* **118,** 8198–8206
15. Parks, M. E., Baird, E. E., and Dervan, P. B. (1996) *J. Am. Chem. Soc.* **118,** 6153–6159
16. Gottesfeld, J. M., Neely, L., Trauger, J. W., Baird, E. E., and Dervan, P. B. (1997) *Nature* 202–205
17. Neely, L., Trauger, J. W., Baird, E. E., Dervan, P. B., and Gottesfeld, J. M. (1997) *J. Mol. Biol.* **274,** 439–445
18. Dickinson, L. A., Gulizia, R. J., Trauger, J. W., Baird, E. E., Mosier, D. E., Gottesfeld, J. M., and Dervan, P. B. (1998) *Proc. Natl. Acad. Sci. U. S. A.* **95,** 12890–12895
19. Tripathy, D., and Benz, C. C. (1993) in *Oncogenes and Tumor Suppressor Gemes in Human Malignancies* (Benz, C. C., and Liu, E., eds) pp. 15–60, Klurwer Academic Publishers, Boston
20. Scott, G. K., Daniel, J. C., Xiong, X., Maki, R. A., Kabat, D., and Benz, C. C. (1994) *J. Biol. Chem.* **269,** 19848–19858
21. Xing, X. M., Wang, S. C., Xia, W. Y., Zou, Y. Y., Shao, R. P., Kwong, K. Y., Yu, Z. M., Zhang, S., Miller, S., Huang, L., and Hung, M. C. (2000) *Nat. Med.* **6,** 189–195
22. Baird, E. E., and Dervan, P. B. (1996) *J. Am. Chem. Soc.* **118,** 6141–6146
23. Brenowitz, M., Senear, D. F., Shea, M. A., and Ackers, G. K. (1986) *Methods Enzymol.* **130,** 132–181
24. White, S., Baird, E. E., and Dervan, P. B. (1996) *Biochemistry* **35,** 12532–12537
25. Chang, C., Scott, G. K., Kuo, W., Xiong, X., Suzdaltseva, Y., Park, J. W., Sayre, P., Erny, K., Collins, C., Gray, J. W., and Benz, C. C. (1997) *Oncogene* **14,** 1617–1622
26. Chang, C. H., Scott, G. K., Baldwin, M. A., and Benz, C. C. (1999) *Oncogene* **18,** 3682–3695
27. Chiang, S. Y., Welch, J., Rauscher, F., III, and Beerman, T. A. (1994) *Biochemistry* **33,** 7033–7040
28. Graves, B. J., Gillespie, M. E., and McIntosh, L. P. (1996) *Nature* **384,** 322
29. Kodandapani, R., Pio, F., Ni, C. Z., Piccialli, G., Klemsz, M., McKercher, S., Maki, R. A., and Ely, K. R. (1996) *Nature* **380,** 456–460
30. Bkosher, J. M., Williams, T., and Hurst, H. C. (1995) *Proc. Natl. Acad. Sci. U. S. A.* **92,** 744–747
31. Nye, J. A., Petersen, J. M., Gunther, C. V., Jonsen, M. D., and Graves, B. J. (1992) *Genes Dev.* **6,** 975–990

Title: Assessing the relationship between DNA-binding agents as inhibitors of Ets-HER2/*neu* promoter complexes and HER2/*neu* transcriptional expression[1].

Authors: Stephanie J. Leslie, Gary K. Scott, Chris C. Benz, and Terry A. Beerman[2]

Department of Molecular Pharmacology and Experimental Therapeutics, Roswell Park Cancer Institute, Buffalo, NY 14263 [S.J.L., T.A.B.]; Department of Cancer and Developmental Therapeutics, Buck Institute for Age Research, Novata, CA 94945 [G.K.S., C.C.B.]

Running Title: Activity of DNA-binding drugs in comparative bioassays.

Key Words: DNA-binding drugs HER2/*neu* promoter-targeted Transcript-inhibiting Growth inhibition Correlation

Footnotes:

[1]This study was supported in part by grants from US Army Medical Research Grants BC980067 (to TAB), DAMD17-98-1-8103 (to SJL), American Cancer Society RPG-96-034-04-CDD (to TAB), NIH CA 36773 and NIH CA58207 (to CCB).

[2]To whom correspondence and reprint requests should be addressed: Terry Beerman, Department of Pharmacology and Therapeutics, Roswell Park Cancer Institute, Elm and Carlton Streets, Buffalo, New York 14263. Tel: 716-845-3443; Fax: 716-845-8857; e-mail: terry.beerman@roswellpark.org

[3]The abbreviations used are: TF, transcription factor; EMSA, electrophoretic mobility shift assay; MGB, minor groove binder; EBS, Ets binding site; IC_{50}, 50% inhibition concentration; GAPDH, glyceraldehyde 3-phosphate dehydrogenase; IC, internal control; SD, standard

deviation.

Abstract:

A strategy for inhibiting gene expression is to utilize DNA-binding compounds that recognize similar DNA binding motifs (based upon sequence and groove preference) as the DNA binding domain of a targeted transcription factor. It is widely assumed that agents found to be potent in reducing complex formation will be effective inhibitors of gene expression or that inhibition of gene expression in cells is a result of drug related interference with the transcription factor/DNA complex. To test the validity of this scheme, drugs with differing DNA-binding motifs (minor groove or intercalating) and sequence preferences (A/T or G/C) were examined for correlations between their ability to inhibit formation of a targeted transcription factor/DNA complex and gene expression. Drug effects on HER2/*neu* promoter binding by ESX, a member of the Ets family of transcription factors, and disruption of the ESX/HER2/*neu* complex were analyzed using a cell-free electrophoretic mobility shift assay. Hoechst 33342, distamycin and hedamycin effectively prevented ESX binding to the HER2/*neu* promoter while chromomycin A_3 was considerably less active. In contrast, in cell-free transcription experiments, chromomycin A_3 was among the most potent inhibitors of HER2/*neu* expression, followed by distamycin and Hoechst 33342, while hedamycin was the least effective. Drug treatment of SK-Br-3 cells, a human breast adenocarcinoma cell line which overexpresses both HER2/*neu* and ESX, revealed hedamycin and chromomycin A_3 to be highly potent inhibitors of HER2/*neu* mRNA transcription while Hoechst 33342 and distamycin were relatively weak inhibitors. Ultimately, the most potent inhibitors of cellular mRNA transcription were the most cytotoxic suggesting that effects on expression were not necessarily directly related to the drug's ability to target the transcription factor/DNA complex. This study points out the need for caution when

extrapolating cell-free evaluations of drugs as inhibitors of transcription factor/DNA complexes to effectiveness as inhibitors of gene expression. Additionally, these results revealed that no agent was capable of selectively inhibiting targeted gene expression. As new generations of more specific DNA binding agents are developed, the use of a linked series of bioassays can help provide validation of the targeting concept.

Introduction:

Agents, which bind preferentially to A/T and G/C sequences, can be targeted to particular gene promoters containing the DNA recognition sequence (1-5). For example, the crescent-shaped DNA minor groove binder (MGB), distamycin, binds preferentially to A/T sequences causing the minor groove to widen and the major groove to narrow (6-9). This agent was found to effectively block formation of TATA box binding protein/DNA complexes (10-13). Similarly, chromomycin A_3, which binds G/C rich regions of DNA within the minor groove, can disrupt transcription factor/DNA complexes due to the significant distortion of the helix that occurs upon its binding (2, 14-17). Chromomycin A_3's effective inhibition of binding by early growth response gene-1 (a G/C-preference major groove binding protein) as well as TATA box binding protein (an A/T-preference minor groove binding protein) are linked to its ability to induce helical alterations that can affect protein binding to either groove (13). Intercalators are another class of DNA-binding agents, which alter DNA conformation by sliding their chromophore between the base pairs of DNA and lengthening the helix (4, 9, 18-21). By altering the positions of donor/acceptor groups that participate in transcription factor (TF) site recognition, intercalators such as hedamycin have been shown to effectively disrupt a variety of TF/DNA complexes including early growth response gene-1, Wilms tumor suppressor gene-1 and TATA box binding protein (12, 13, 22).

While it is apparent that TF DNA-binding domains can be targeted by DNA-binding drugs, whether the disruption of the TF promoter complex, inhibition of gene expression, and cellular response are linked is less clear. In fact, differing results have been observed when drug-induced inhibition of TF binding to promoter response elements and inhibition of gene

expression in both cell-free and whole cell assays is compared (22-25). Also, a recent study suggested that for some DNA-binding drugs a decrease in cellular gene expression is more likely associated with general cytotoxicity than with targeted gene inhibition (26).

The present study compared agents with differing DNA-binding specificities to inhibit formation of TF complexes on a key gene regulatory element. Drug affects in cell-free assays (EMSA and *in vitro* transcription) are compared to RNA expression and growth inhibition of a cultured human breast cancer cell line (SK-Br-3). The viability and proliferation of SK-Br-3 cells depends on overexpression of the HER2/*neu* (ErbB2) oncogene, which requires an intact Ets binding site (EBS) (27-34). This EBS (GAGGAAGT) can be targeted by either A/T or G/C sequence specific agents. The four DNA-binding antibiotics examined in this study include the A/T sequence preferring minor groove binding agents distamycin and Hoechst 33342, the G/C sequence preferring minor groove-binding agent chromomycin A_3, and the G/C sequence preferring intercalator hedamycin. Whether the potency of sequence specific DNA-reactive agents as inhibitors of TF/DNA complexes in cell-free assays is predictive of their ability to modulate TF function in both cell-free and cellular environments was determined.

Materials & Methods:

Drugs:

Hedamycin (5 mM), supplied by the National Cancer Institute, was prepared by dissolving in 1/10 volume 0.1 N HCl, adding 8/10 volume ddH_2O, and neutralizing with 1/10 volume 0.1 N sodium hydroxide. Stocks of distamycin (5 mM; Sigma, St. Louis, MO) and Hoechst 33342 (20 mM; Aldrich, Chemical Co., Milwaukee, WI) were prepared in ddH_2O. Chromomycin A_3 (5 mM; Sigma, St. Louis, MO) was prepared in dimethylsulfoxide. All drug stocks were stored at –20°C and diluted into water immediately before use.

Cell Culture:

HER2/*neu*-amplified and -overexpressing SK-Br-3 cells (human breast adenocarcinoma) were purchased from American Tissue Culture Collection (Rockville, MD) and grown in McCoy's 5a medium (GIBCO, Grand Island, NY) with 10% fetal bovine serum. Cells were sub-cultured after reaching ~80% confluence ($1x10^7$ cells/T75 dish) by resuspending in medium and plating at $3x10^5$ cells/ml.

Electrophoretic Mobility Shift Assay (EMSA):

A bacterially expressed Ets protein, ESX, known to bind to the HER2/*neu* promoter's EBS, was prepared as previously described (31, 35). Briefly, a full-length ESX cDNA was cloned into a pRSET Histidine-tag expression plasmid (NheI-HindIII; Invitrogen) and expressed in isopropylthio-β-D-galatoside induced BL21[DE3] pLysS bacteria (Stratagene, La Jolla, CA). Histidine-tagged ESX protein was purified from the bacteria by Nickel-chelate affinity

chromatography, as recommended by the manufacturer (Qiagen Inc., Valencia, CA). A 34-mer oligonucleotide (TA5-34 oligo), 5'-GGAGGAGGAGGGCTGCTT GAGGAAGTATAAGAAT-3', containing the EBS (underlined sequence), derived from the HER2/*neu* gene promoter and its complementary strand were synthesized by the Biopolymer facility (Roswell Park Cancer Institute, Buffalo, NY). The oligonucleotide was purified, annealed and end-labeled with [γ-^{32}P]-ATP using T4-polynucleotide kinase (New England BioLabs, Beverly, MA), as described previously (12, 35). For optimization of EMSA conditions, full-length ESX protein was titrated in the presence of ^{32}P-end labeled TA5-34 oligonucleotide (1 nM) in binding buffer (30 mM potassium chloride, 5% glycerol, 25 mM Tris [pH 7.5], 0.1% NP-40, 0.1 mg/ml bovine serum albumin and 1 mM dithiothreitol). Maximal ESX/DNA complex formation (~90%) was achieved at 40 nanograms of ESX protein. A 30-minute incubation at room temperature was sufficient time to achieve equilibrium between ESX and the oligonucleotide (35). Following complex formation, samples were electrophoresed for 60 minutes at 200 volts on a 4% polyacrylamide gel using 0.5X TBE buffer (44.5 mM Tris base, 44.5 mM boric acid, 1.0 mM ethylenediamine tetraacetic acid [pH 8.0]). Gels were dried and exposed to Kodak Biomax Scientific Imaging film. A Molecular Dynamics densitometer (Molecular Dynamics, Sunnyvale, CA) was used for quantitation of EMSA TF/DNA complexes and images were analyzed using ImageQuant software. The drugs' ability to disrupt the ESX/DNA complex formation was assessed by 30-minute pre-incubation of the oligonucleotide with drug, prior to the 30-minute incubation of the probe with the recombinant ESX protein and EMSA. Percent inhibition of complex formation by drug was determined by comparing the signal intensity of complex in drug-treated samples to that generated by 4 untreated controls, and

IC_{50} values (amount of drug needed to inhibit 50% of complex formation) for all agents were determined.

Cell-free transcription assay:

Cesium chloride-purified plasmid DNA (RO6), containing a ~500 bp insert DNA fragment from the HER2/*neu* promoter fragment in the reporter gene expression construct pCDNA3-Luc (Invitrogen, Carlsbad, CA), was linearized with restriction enzyme, *SphI* (New England BioLabs, Beverly, MA) (36). Nuclear extract was prepared as described previously from SK-Br-3 cells, which overexpress both HER2/*neu* and various Ets factors including ESX (35).

Radiolabeled transcripts were generated by incubation of DNA template and SK-Br-3 nuclear extract for 60 minutes in labeling cocktail containing [α-^{32}P]-CTP (800Ci/mmole; NEN, Boston, MA). Samples were extracted and electrophoresed under conditions described by Chiang et al. (35). A PhosphorImager screen was used to visualize the ^{32}P signal from dried gels and the signal was quantified using a Molecular Dynamics PhosphorImager. T3 transcript (250 bases; Promega Co., Madison, WI) was used as an internal loading control for each sample. An RNA ladder (Gibco BRL, Grand Island, NY) of 1.77 – 0.155 kilobase pairs was dephosphorylated, end-labeled and purified as described previously and was used to verify the band of interest based on an expected HER2/*neu* transcript size of ~760 base pairs (35). Nuclear extract was titrated in the presence of a constant amount of plasmid DNA (1 μg) to obtain the optimal signal for the 760 base pair HER2/*neu* transcript.

Inhibition of Ets-regulated gene expression was assessed by incubation of the drug with the DNA template in reaction buffer for 30 minutes at 30°C prior to addition of labeling cocktail with the Ets-containing, including ESX, SK-Br-3 nuclear extract. ImageQuant signal intensity of the HER2/*neu* reporter gene transcript (luc) for control and drug treated samples were normalized to the internal loading control signal. For each agent the percent inhibition of transcript formation was determined by comparing the drug-treated normalized HER2/*neu* transcript signal to that of 4 normalized untreated control HER2/*neu* transcript signals. IC_{50} values for each agent was also determined.

Northern Blot Analysis:

SK-Br-3 cells (5×10^5) were plated in 60 mm dishes. 72 hours after plating, the medium was changed followed by drug addition at the indicated concentrations. At the times indicated after drug treatment, total RNA was harvested from the cells using TRIzol Reagent (GIBCO, Grand Island, NY), as recommended by the manufacturer. Equal amounts (based upon absorbance at 260nm) of total RNA from each sample were electrophoresed for 4.5 hours at 80 volts on a 1.5% agarose-formaldehyde gel (40 mM 3-(N-morpholino)-propanesulfonic acid [pH 7.0], 10 mM sodium acetate, 10 mM ethylenediamine tetraacetic acid and 2.2 M formaldehyde) with a buffer containing 40 mM 3-(N-morpholino)-propanesulfonic acid, pH 7.0, 10 mM sodium acetate, 10 mM ethylenediamine tetraacetic acid. The gel was then transferred overnight to a nylon membrane (Genescreen, NEN Life Science Products, Boston, MA). Following UV cross-linking, the membrane was placed in a hybridization bottle with pre-hybridization buffer (0.5 M sodium phosphate, pH 7.2, 7% sodium dodecyl sulfate, 1 mM ethylenediamine tetraacetic acid,

1% bovine serum albumin) at 60°C for 60 minutes. The membrane was then hybridized overnight with [α-^{32}P]-CTP radiolabeled HER2/*neu* cDNA (pBluescript, 1.5Kb *EcoRI* fragment) and [α-^{32}P]-CTP radiolabeled glyceraldehyde 3-phosphate dehydrogenase cDNA (American Type Culture Collection, pBluescript SK$^-$, 1.2Kb *EcoRI* fragment). The hybridized membrane was washed twice for 20 minutes at 60°C with 40 mM sodium phosphate, pH 7.2, 5% sodium dodecyl sulfate, 1 mM ethylenediamine tetraacetic acid, and 0.5 % bovine serum albumin, followed by two additional washes for 20 minutes at 60°C with 20 mM sodium phosphate, pH 7.2, 1% sodium dodecyl sulfate and 1 mM ethylenediamine tetraacetic acid. Blots were exposed to a PhosphorImaging Screen and the ^{32}P signal of both HER2/*neu* and GAPDH transcript signals were quantitated by a Molecular Dynamics PhosphorImager and analyzed with ImageQuant software. The assessment of drug inhibition of gene expression was determined by dividing the signal of the mRNA bands from drug treated samples by the average mRNA signal generated by 4 untreated control samples.

Results:

Effects of DNA-binding agents on formation of the ESX/HER2/*neu* promoter complex.

DNA-binding agents (structures presented in Figure 1A) with varying binding motifs were evaluated by EMSA for their efficacy at preventing the binding of a purified recombinant Ets protein, ESX, to the HER2/*neu* promoter. An oligonucleotide probe (Figure 1B) containing the EBS consensus-binding site from the HER2/*neu* promoter was incubated with purified ESX and reactions were resolved on a native polyacrylamide gel. A representative EMSA is presented in Figure 2A. Pre-incubating varying drug concentrations with the DNA probe prior to the addition of ESX, as shown for Hoechst 33342 in Figure 2A, inhibited ESX/DNA complex formation in a concentration-dependent manner. For Hoechst 33342 complete inhibition of ESX/DNA complexes was seen at a concentration of 4.0 μM with 50% inhibition at 1.4 μM. Results for each of the DNA-binding agents tested are shown graphically in Figure 2B and their IC_{50} values summarized in Table 1. Comparison of the IC_{50} values of the two A/T preferring drugs, distamycin and Hoechst 33342 (0.7 μM and 1.4 μM, respectively), indicated these agents were similarly effective in preventing complex formation. The G/C preferring intercalator, hedamycin, had the lowest IC_{50} value (0.5 μM) with close to complete inhibition observed at 1.0 μM (Figure 2B). The evaluation of chromomycin A_3 was complicated by the fact that 12 mM Mg^{+2} is needed for optimal chromomycin A_3 binding to DNA and at these levels the ESX/DNA complex was reduced in the absence of drug. A maximal Mg^{+2} concentration of 5 mM was chosen which retained ~60% of the ESX/DNA complex compared with controls without Mg^{+2} (data not shown). These sub-optimal concentrations of Mg^{+2} likely contributed to the relatively

high IC_{50} value of 10 μM (as per Table 1A) for ESX/DNA complex inhibition and the fact that it could not completely inhibit the ESX/DNA complex even up to 20 μM, the highest concentration tested (Figure 2B).

Effects of DNA-binding agents on cell-free expression of HER2/*neu*.

The agents studied in EMSAs were next evaluated for their efficacy as inhibitors of Ets and/or TBP initiated cell-free transcription of the HER2/*neu* promoter template. This assay provides a more complex environment for drug evaluation compared with EMSAs since it includes many other nuclear components and uses a relatively large, linearized plasmid DNA target that contains the HER2/*neu* promoter and luciferase template. Briefly, plasmid was incubated for 1 hour with nuclear extracts from SK-Br-3 cells and [α-^{32}P]-CTP. The radiolabeled transcripts were resolved on a denaturing polyacrylamide gel along with an RNA ladder to identify the major HER2/*neu* band (~760 base pairs) of interest (35).

DNA-binding agents were incubated with the DNA template prior to transcript formation to assess drug effectiveness as an inhibitor of cell-free expression from the HER2/*neu* promoter. Figure 3 shows representative data demonstrating the concentration-dependent inhibition of HER2/*neu* transcript formation by Hoechst 33342. About 95% inhibition of HER2/*neu* transcript formation was observed at 10 μM (lane 2) while detectable inhibition is seen at a concentration as low as 2.5 μM (lane 4). The Hoechst 33342 IC_{50} value in the assay is 3.0 μM (Table 1A). The average levels of inhibition were derived from a quantitative analysis of more than six separate experiments which are not always fully reflected in the individual gel image.

Results of cell-free transcription assays performed for each agent are presented in Figure 4 with IC_{50} values listed in Table 1A. Like the EMSA studies, A/T sequence preferring drugs, distamycin and Hoechst 33342, showed similar IC_{50} values of 3.0 μM (Figure 4). Detectable inhibition by distamycin was seen at a concentration of 2.5 μM with complete inhibition by 10 μM. Contrary to being the most effective agent in the EMSA analysis, the G/C intercalator, hedamycin, was the least potent inhibitor of cell-free transcription, requiring 25 μM to reach ~90% inhibition. While optimal drug-DNA binding conditions could not be achieved in the EMSAs for chromomycin A_3, the nuclear extract containing transcription conditions, which included higher Mg^{+2} concentrations, likely allowed for more effective binding of chromomycin A_3 to the promoter template. Under these assay conditions, chromomycin A_3 was the most potent HER2/*neu* transcript inhibitor with detectable inhibition by 1.0 μM, an IC_{50} of 1.5 μM and maximal inhibition by 5.0 μM (Figure 5). Consistent with the concentration-dependent decrease in the major HER2/*neu* transcript (760 base pairs), we noted a concentration-dependent drug induced increase in partial transcript production in some samples suggesting an additional effect on transcript elongation (in Figure 3 lanes 2 to 5 the decreased 760 base pair full-length band is accompanied by an increase in partial transcripts located below the 280 base pair marker and just above the internal control in each lane).

Effects of DNA-binding agents on HER2/*neu* cellular mRNA levels in SK-Br-3 cells.

Despite the utility in using simplistic cell-free assays such as EMSA and *in vitro* transcription for evaluating drugs, ultimately whole cell assessment is needed to determine their overall effectiveness and target specificity. Northern blot analysis of cells treated 24 hours with

each DNA-binding agent was used to determine their ability to inhibit endogenous HER2/*neu* transcription. SK-Br-3 cells, whose viability depends on HER2/*neu* overexpression, were used in these studies. GAPDH (glyceraldehyde 3-phosphate dehydrogenase), a housekeeping gene with comparable mRNA half-life with that of HER2/*neu* mRNA (~8h), was used to measure the overall effects on the cell's transcriptional machinery (37, 38). Figure 5A shows a representative Northern blot and the concentration-dependent inhibition of HER2/*neu* mRNA levels by Hoechst 33342. Detectable inhibition was seen at 5.0 μM (lane 4) with a resulting Hoechst IC_{50} of 9.0 μM (Figure 5B and Table 1B). In comparison, GAPDH mRNA was also inhibited to comparable levels as HER2/*neu* following Hoechst 33342 treatment (Figure 5). Northern blots were performed for each of the other drugs (Figure 5) with IC_{50} values presented in Table 1B.

Since cellular uptake and stability may affect drug action and the inhibition of HER2/*neu* and GAPDH transcripts may have different time dependencies, the time-dependent effects on inhibition of mRNA levels were evaluated. The standard assay used a 24-hour time point to allow for the relatively long half-lives of HER2/*neu* and GAPDH. To determine if longer time points might alter the relative transcript inhibiting results, the least cytotoxic agent, distamycin (see Table 1B), was studied since long-term treatment by the other drugs resulted in significant losses in recoverable total RNA. Northern blot analysis was performed on total RNA harvested from SK-Br-3 cells treated with 50 μM distamycin for 24, 48, and 72 hours. As shown in Figure 5 there was a time-dependent decrease in HER2/*neu* mRNA levels that was not significantly different from that of the GAPDH mRNA inhibition.

Effects of DNA-binding agents on SK-Br-3 cell growth.

While all agents tested in Northern blot analysis inhibited HER2/*neu* mRNA production, more than two orders of magnitude differences were observed in drug potency. These differences could result from diverse levels of specificity for the HER2/*neu* promoter or from dissimilar specificities on other essential genes or the general transcriptional machinery. Thus, each agent was evaluated for the ability to inhibit SK-Br-3 cell growth over a 72-hour continuous exposure. Cell growth inhibition was determined by comparing the cell count of drug-treated samples with the cell count of untreated controls and IC_{50} values are presented in Table 1B. Hedamycin and chromomycin A_3 had IC_{50} values in the sub-micromolar concentration range while the Hoechst 33342 IC_{50} value was in the low micromolar range. Distamycin was clearly the least cytotoxic having an IC_{50} concentration in the hundred-micromolar range. The two agents that were most potent at inhibiting HER2/*neu* and GAPDH mRNA levels, chromomycin A_3 and hedamycin, were also the most potent inhibitors of cell growth. Likewise, for Hoechst 33342 and distamycin, there was a similarity between intracellular mRNA transcription (i.e. Northern blots) and the ability to inhibit cell growth, with Hoechst 33342 being more effective than distamycin in both assays.

Discussion:

Despite understanding the mechanisms by which TFs regulate gene expression at the molecular level, utilization of this information to design inhibitors has lagged. This study assessed the strategy of inhibiting gene expression by targeting DNA-binding agents to a transcription factor binding site on a gene promoter in order to disrupt complex formation. Drugs used as gene expression inhibitors are often based upon their inhibitory activity in EMSA assays,

which utilizes a purified TF and a small oligonucleotide containing just the TF consensus-binding site. However, results from EMSA studies may not be predictive of drug performance as an inhibitor of expression where regulation involves the interaction of numerous factors within a relatively large gene promoter region. This study not only analyzed drugs for their ability to inhibit the Ets transcription factor, ESX, from binding to its consensus DNA site but also examined whether this ability corresponded to subsequent effects on cell-free and cellular expression of an Ets-regulated gene (HER2/*neu*).

All agents were initially examined in a cell-free EMSA assay and found to inhibit ESX/HER2/*neu* promoter complex formation in a dose-dependent manner with an overall order of potency hedamycin = distamycin > Hoechst 33342 >> chromomycin A_3. Based upon hedamycin's intercalative mode of DNA-binding, its potency as an inhibitor is likely related to its ability to create significant distortion of the DNA helix with loss of binding site recognition by ESX (2, 9, 19, 39, 40). The minor groove binding agents, distamycin and Hoechst 33342 may also effectively inhibit ESX/HER2/*neu* promoter complex formation by directly competing with ESX for binding to minor groove contacts within its DNA-binding domain. Distamycin's slightly increased efficiency compared with Hoechst 33342, may be due to its capacity to bind as a side-by-side dimer in regions with at least five A/T base pairs resulting in further narrowing of the major groove thus interfering with ESX binding to its major groove contacts (2, 6-9, 41). Chromomycin A_3 was the least effective inhibitor of ESX/HER2/*neu* promoter complex formation likely due to the use of sub-optimal concentrations of Mg^{+2}, an ion that is required by chromomycin A_3 for DNA-binding. These results contrast with its observed potent inhibition ($\leq$

1 μM) of other TF/DNA complexes such as early growth response gene-1, Wilms tumor suppressor gene-1 and TATA box binding protein (13).

Whether agents that blocked ESX/DNA complex formation also inhibit Ets-regulated gene expression were evaluated utilizing cell-free expression assays containing an exogenous DNA source in the presence of a nuclear lysate that includes functional transcriptional machinery and endogenous factors including ESX. All agents tested showed a capacity to inhibit cell-free transcription, while in contrast to the EMSA findings, the order of potency of the G/C preferring agents differed, with chromomycin A_3 being the most potent and hedamycin the least: chromomycin A_3 > distamycin = Hoechst 33342 > hedamycin (Table 1A).

Chromomycin A_3's increased efficacy is likely due in part to the enhanced DNA-binding conditions created by the higher concentrations of Mg^{+2} (~7.5 mM), allowing for the formation of the Mg^{+2}-coordinated head-to-tail chromomycin A_3 dimers. That these dimers create significant distortion and opening of the minor groove upon binding to the DNA could contribute to chromomycin A_3's enhanced efficacy (9). In contrast, hedamycin, a potent inhibitor of ESX/HER2/*neu* complex formation, showed relatively weak inhibition of HER2/*neu* transcript formation. It is not clear why hedamycin's efficacy decreased so dramatically since previously our lab found hedamycin to be an effective inhibition of E2F-dependent cell-free expression (22). Possibly hedamycin binds at sufficient distances form the transcriptional machinery that the distortion caused by intercalation does not interfere with the transcriptional process. In contrast to chromomycin A_3 and hedamycin, which cause significant helical distortions, distamycin and Hoechst 33342 only produce minimal topological effects on the DNA helix. Distamycin and Hoechst 33342 were equally inhibitory to HER2/*neu* transcript formation and demonstrated

limited correlation with the EMSA results. Since these two agents share similar DNA-binding motifs, they would likely target common TF/DNA complexes such as the TATA box binding protein.

From the prospective of the template and transcriptional machinery, inhibition of *in vitro* transcription cannot be attributed exclusively to inhibition of ESX binding since other Ets proteins found in the nuclear extract or other proteins involved in HER2/*neu* regulation could be inhibited. Alternatively, decreased transcription could be due to inhibition of binding by basal TFs, such as TATA box binding protein, rather than the prevention of specific Ets protein binding. An effect on general transcriptional machinery rather than targeted inhibition of Ets binding by the MGBs is further supported by the appearance of partial HER2/*neu* transcripts.

Inhibition of cell-free and cellular expression might differ since the latter requires drug access to the nuclear target and stability in a cellular environment. Northern blot analysis revealed a concentration-dependent inhibition of cellular HER2/*neu* mRNA levels with the following potency order: chromomycin A_3 > hedamycin >> Hoechst 33342 >> distamycin. Significantly, only chromomycin A_3 behaved similarly as an inhibitor of cell-free and cellular expression. Also, only the agents inducing significant helical distortions (chromomycin A_3 and hedamycin) were potent inhibitors of cellular HER2/*neu* expression. Drug induced helical distortion could decrease HER2/*neu* transcription by inhibiting the general transcriptional machinery, which is necessary for optimizing expression.

Investigation of drug effects on SK-Br-3 cell growth revealed the same order of potency as observed for northern blot analysis: chromomycin A_3 > hedamycin >> Hoechst 33342 >> distamycin. While the expression data provided fairly specific information about drug effects on

a gene target, other non-specific effects in cells can influence cytotoxicity data. For example, the longer time periods utilized in the cell growth inhibition studies will be influenced by drug stability within the cellular environment. In addition, studies have shown some cell lines actively remove Hoechst 33342 (42, 43). Similarly, cellular uptake might influence cytotoxicity results.

This study revealed the difficulty in extrapolating a drug's ability to inhibit cell-free TF/DNA complex formation to its effectiveness as an inhibitor of both cell-free and cellular gene expression. While each of these assays provide consistent evidence of drug inhibition of TF binding they cannot take into account factors in a whole cell environment that may impinge upon drug activity. Extrapolation of the cellular mRNA inhibition to equally cytotoxic drug levels revealed no agent capable of selectively inhibiting targeted gene expression. Likewise, attempts at correlating TF/DNA complex formation with cellular gene expression and cytotoxicity is difficult since we cannot ascertain if cell death was due to HER2/*neu* inhibition or to some other drug associated event.

Drug effects on expression in cells may or may not be strictly related to the ability of the drug to target a particular gene promoter. Understanding the mechanism of molecular regulation of a gene promoter and cell-free evaluation of how drugs can affect the individual components of this regulation are needed to develop drugs with enhanced inhibitory activity. There is a need for further development of drugs that cannot only inhibit gene expression in cells, but can do so in a manner that is based upon a DNA targeting strategy. Recent studies have found that uniquely designed sequence specific minor groove binding agents, polyamides, which are not cytotoxic, bind DNA as side-by-side dimers and are extremely effective inhibitors of TF/DNA complex formation and cell-free expression (44-50). Effective inhibition of ESX binding to the HER2/*neu*

promoter as well as inhibition of Ets-regulated cell-free expression by polyamides also was reported (35). Currently, studies are underway to develop polyamides as more specific inhibitors of HER2/*neu* expression in cells without the accompanying whole-cell cytotoxicity, which often occurs with the more conventional DNA-binding agents.

1. Waring, M. J. and Bailly, C. DNA recognition by intercalators and hybrid molecules, Journal of Molecular Recognition. *7:* 109-22, 1994.
2. Yang, X. L. and Wang, A. H. Structural studies of atom-specific anticancer drugs acting on DNA, Pharmacol Ther. *83:* 181-215, 1999.
3. Neidle, S. Crystallographic insights into DNA minor groove recognition by drugs, Biopolymers. *44:* 105-121, 1997.
4. Chaires, J. B. Energetics of drug-DNA interactions, Biopolymers. *44:* 201-15, 1997.
5. Ren, J. and Chaires, J. B. Sequence and structural selectivity of nucleic acid binding ligands, Biochemistry. *38:* 16067-75, 1999.
6. Pelton, G. and Wemmer, D. E. Structural characterization of a 2:1 distamycin A d(CGCAAATTGGC) complex by two dimensional NMR, Proc Natl Acad Sci USA. *86:* 5723-5727, 1989.
7. Chen, X., Ramakrishnan, B., Rao, S. T., and Sundaralingam, M. Binding of two distamycin A molecules in the minor groove of an alternating B-DNA duplex, Nature Structural Biology. *1:* 169-75, 1994.
8. Chen, X., Ramakrishnan, B., and Sundaralingam, M. Crystal structures of the side-by-side binding of distamycin to AT-containing DNA octamers d(ICITACIC) and d(ICATATIC), Journal of Molecular Biology. *267:* 1157-70, 1997.
9. Geierstanger, B. H. and Wemmer, D. E. Complexes of the minor groove of DNA, Annu Rev Biophys Biomol Struct. *24:* 463-493, 1995.
10. Bellorini M, M. V., D'Incalci M, Mongelli N, Mantovani R Distamycin A and tallimustine inhibit TBP binding and basal in vitro transcription., Nucleic Acids Res. *23:* 1657-63, 1995.
11. Chiang, Y.-S., Welch, J. J., Rauscher, F., and Beerman, T. A. Effect of DNA Binding Drugs on EGR1 and TBP Complex Formation with the Herpes Simplex Virus Latency Promoter, J. Biol. Chem. *271:* 23999-24004, 1996.
12. Chiang, S. Y., Welch, J., Rauscher, F. J., 3rd, and Beerman, T. A. Effects of minor groove binding drugs on the interaction of TATA box binding protein and TFIIA with DNA, Biochemistry. *33:* 7033-40, 1994.

13. Welch, J. J., Rauscher, F. J., 3rd, and Beerman, T. A. Targeting DNA-binding drugs to sequence-specific transcription factor/DNA complexes. Differential effects of intercalating and minor groove binding drugs, J Biol Chem. *269:* 31051-8, 1994.

14. Gao, X. L., Mirau, P., and Patel, D. J. Structure refinement of the chromomycin dimer-DNA oligomer complex in solution, J Mol Biol. *223:* 259-79, 1992.

15. Sastry, M. and Patel, D. J. Solution structure of the mithramycin dimer-DNA complex, Biochemistry. *32:* 6588-604, 1993.

16. Sastry, M., Fiala, R., Lipman, R., Tomasz, M., and Patel, D. J. Solution structure of the monoalkylated mitomycin C-DNA complex, J Mol Biol. *247:* 338-359, 1995.

17. Keniry, M. A., Banville, D. L., Simmonds, P. M., and Shafer, R. Nuclear magnetic resonance comparison of the binding sites of mithramycin and chromomycin on the self-complementary oligonucleotide d(ACCCGGGT)2. Evidence that the saccharide chains have a role in sequence specificity, Journal of Molecular Biology. *231:* 753-67, 1993.

18. Searle, M. NMR Studies of Drug-DNA Interactions., Progress in NMR Spectroscopy. *25:* 403-80, 1993.

19. Sun, D., Hansen, M., Clement, J. J., and Hurley, L. H. Structure of the altromycin B (N7-guanine)-DNA adduct. A proposed prototypic DNA adduct structure for the pluramycin antitumor antibiotics, Biochemistry. *32:* 8068-74, 1993.

20. Gago, F. Stacking interactions and intercalative DNA binding, Methods. *14:* 277-92, 1998.

21. Neidle S, A. Z. Structural and sequence-dependent aspects of drug intercalation into nucleic acids., CRC Crit Rev Biochem. *17:* 73-121, 1984.

22. Chiang, S. Y., Azizkhan, J. C., and Beerman, T. A. A comparison of DNA-binding drugs as inhibitors of E2F1- and Sp1-DNA complexes and associated gene expression, Biochemistry. *37:* 3109-15, 1998.

23. Snyder, R. C., Ray, R., Blume, S., and Miller, D. M. Mithramycin blocks transcriptional initiation of the c-myc P1 and P2 promoters, Biochemistry. *30:* 4290-4297, 1991.

24. Ray R, S. R., Thomas S, Koller CA, Miller DM Mithramycin blocks protein binding and function of the SV40 early promoter., J Clin Invest. *83:* 2003-7, 1989.

25. Miller, D. M., Polansky, D. A., Thomas, S. D., Ray, R., Campbell, V. W., Sanchez, J., and Koller, C. A. Mithramycin selectively inhibits transcription of G-C containing DNA, American Journal of the Medical Sciences. *294:* 388-94, 1987.

26. White, C. M., Heidenreich, O., Nordheim, A., and Beerman, T. A. Evaluation of the Effectiveness of DNA-Binding Drugs To Inhibit Transcription Using the c-fos Serum Response Element as a Target, Biochemistry. *39:* 12262-12273, 2000.

27. Ets Gene Family, Oncogene. *19:* 6393-6548, 2000.

28. Scott, G., Chang, C.-H., Erny, K., Xu, F., Fredericks, W., III, F. R., Thor, A., and Benz, C. Ets Regulation of the erbB2 Promoter., Oncogene. *19:* 6490-6502, 2000.

29. Klapper, L. N., Kirschbaum, M. H., Sela, M., and Yarden, Y. Biochemical and clinical implications of the ErbB/HER signaling network of growth factor receptors, Advances in Cancer Research. *77:* 25-79, 2000.

30. Graves, B. J. and Petersen, J. M. Specificity within the ets family of transcription factors, Adv Cancer Res. *75:* 1-55, 1998.

31. Chang, C. H., Scott, G. K., Kuo, W. L., Xiong, X., Suzdaltseva, Y., Park, J. W., Sayre, P., Erny, K., Collins, C., Gray, J. W., and Benz, C. C. ESX: a structurally unique Ets overexpressed early during human breast tumorigenesis, Oncogene. *14:* 1617-22, 1997.

32. Roh, H., Pippin, J., Green, D., Boswell, C., Hirose, C., Mokadam, N., and Drebin, J. HER2/neu antisense targeting of human breast carcinoma., Oncogene. *19:* 6138-6143, 2000.

33. Neve, R., Nielsen, U., Kirpotin, D., Poul, M.-A., Marks, J., and Benz, C. Biological effects of anti-ErbB2 single chain antibodies selected for internalizing function., Biochemica & Biophysica Research Communication. *280:* 274-279, 2001.

34. Benz, C. and Tripathy, D. ErbB2 overexpression in breast cancer: biology and clinical translation., Journal of Women's Cancer. *2:* 33-40, 2000.

35. Chiang, S. Y., Burli, R., Benz, C. C., Gawron, L. S., Scott, G. K., Dervan, P. B., and Beerman, T. A. Targeting the Ets Binding Site of the HER2/neu Promoter with Pyrrole-Imidazole Polyamides, Journal of Biological Chemistry. *275:* 24246-24254, 2000.

36. Scott, G. K., Daniel, J. C., Xiong, X., Maki, R. A., Kabat, D., and Benz, C. C. Binding of an ETS-related Protein within the DNase I Hypersensitive Site of the HER2/neu Promoter in Human Breast Cancer Cells, J. Biol. Chem. *269:* 19848-19858, 1994.

37. Dani, C., Piechaczyk, M., Audigier, Y., El Sabouty, S., Cathala, G., Marty, L., Fort, P., Blanchard, J. M., and Jeanteur, P. Characterization of the transcription products of glyceraldehyde 3-phosphate-dehydrogenase gene in HeLa cells, European Journal of Biochemistry. *145:* 299-304, 1984.

38. Pasleau, F., Grooteclaes, M., and Gol-Winkler, R. Expression of the c-erbB2 gene in the BT474 human mammary tumor cell line: measurement of c-erbB2 mRNA half-life, Oncogene. *8:* 849-54, 1993.

39. Henderson, D. and Hurley, L. H. Specific targeting of protein-DNA complexes by DNA-reactive drugs (+)-CC-1065 and pluramycins, Journal of Molecular Recognition. *9:* 75-87, 1996.

40. Pavlopoulos, S., Bicknell, W., Craik, D. J., and Wickham, G. Structural characterization of the 1:1 adduct formed between the antitumor antibiotic hedamycin and the oligonucleotide duplex d(CACGTG)2 by 2D NMR spectroscopy, Biochemistry. *35:* 9314-24, 1996.

41. Wemmer, D., Geierstanger, B., Fagan, P., Dwyer, T., Jacobsen, J., Pelton, J., Ball, G., Leheny, A., Chang, W.-H., Bathini, Y., Lown, J., Rentzeperis, D., Marky, L., Singh, S., and Kollman, P. Minor Groove Recognition of DNA by Distamycin and Its Analogs. *In:* R. Sarma and M. Sarma (eds.), Structural Biology: The State of the Art, pp. 301-323. Schenectady: Adenine Press, 1994.

42. Levina, V. V., Varfolomeeva, E. Y., and Filatov, M. V. "DNA clearing" from non-covalently bound agents in mammalian cells as a new mechanism of drug resistance, Membr Cell Biol. *12:* 883-93, 1999.

43. Filatov, M. V. and Varfolomeeva, E. Y. Active dissociation of Hoechst 33342 from DNA in living mammalian cells, Mutat Res Fundam Mol Mech Mutagen. *327:* 209-215, 1995.

44. Dickinson, L. A., Trauger, J. W., Baird, E. E., Dervano, P. B., Graves, B. J., and Gottesfeld, J. M. Inhibition of Ets-1 DNA binding and ternary complex formation

between Ets-1, NF-kappaB, and DNA by a designed DNA-binding ligand, J Biol Chem. *274:* 12765-12773, 1999.

45. Dickinson, L. A., Trauger, J. W., Baird, E. E., Ghazal, P., Dervan, P. B., and Gottesfeld, J. M. Anti-repression of RNA polymerase II transcription by pyrrole-imidazole polyamides, Biochemistry. *38:* 10801-7, 1999.

46. Dickinson, L. A., Gulizia, R. J., Trauger, J. W., Baird, E. E., Mosier, D. E., Gottesfeld, J. M., and Dervan, P. B. Inhibition of RNA polymerase II transcription in human cells by synthetic DNA-binding ligands [see comments], Proceedings of the National Academy of Sciences of the United States of America. *95:* 12890-5, 1998.

47. Gottesfeld, J. M., Neely, L., Trauger, J. W., Baird, E. E., and Dervan, P. B. Regulation of gene expression by small molecules, Nature. *387:* 202-5, 1997.

48. Bailly, C. and Chaires, J. B. Sequence-specific DNA minor groove binders. Design and synthesis of netropsin and distamycin analogues, Bioconjugate Chemistry. *9:* 513-38, 1998.

49. Chaires, J. B. Drug--DNA interactions, Current Opinion in Structural Biology. *8:* 314-20, 1998.

50. Walker, W. L., Kopka, M. L., and Goodsell, D. S. Progress in the design of DNA sequence-specific lexitropsins, Biopolymers. *44:* 323-334, 1997.

Table 1: IC50 values for each agent tested in cell-free and whole-cell assays. ***A***, the DNA binding agents are listed below with their respective DNA binding properties and IC_{50} values for inhibition of ESX/DNA complex formation in electrophoretic mobility shift assays and HER2/*neu* transcript formation in cell-free transcription assays. ***B***, each agent was evaluated for ability to inhibit HER2/*neu* and GAPDH mRNA production following a 24-hour drug exposure using northern blot analysis. Comparing the cell count of SK-Br-3 cells following a 72-hour continuous drug exposure to the cell count of untreated controls yielded cell growth inhibition values.

A.

Drug	EMSA IC_{50} values (μM)	Cell-free transcription IC_{50} values (μM)
Hoechst 33342	1.4	3.0
Distamycin A	0.7	3.0
Chromomycin A_3	10.0	1.5
Hedamycin	0.5	8.0

B.

Drug	Northern blots (24 hrs) IC_{50} values (μM)		Cell Growth Inhibition (72 hrs) IC_{50} values (μM)
	HER2/*neu*	GAPDH	
Chromomycin A_3	0.04	0.07	0.05
Hedamycin	0.21	0.21	0.10
Hoechst 33342	9	9	7.0
Distamycin A	66	57	114

Figure 1: ***A,*** structures of the DNA binding agents. ***B***, partial HER2/*neu* promoter sequence containing the ESX binding site (bold) and the EBS core sequence (underline). There is also a TBP binding site overlapping the 3'-end of the ESX binding site.

Figure 2: Inhibition of ESX binding to the HER/*neu* promoter by each DNA-binding agents. ***A***, Hoechst 33342 (0-4 μM) was incubated with ^{32}P-labeled oligonucleotide containing a portion of the HER2/*neu* promoter followed by incubation with purified bacterial-expressed ESX protein. Samples were electrophoresed on 4% native polyacrylamide gels, dried, exposed to film and inhibition of ESX/DNA complex formation quantitated by densitometric analysis. The figure shows a representative EMSA demonstrating the concentration-dependent ability of Hoechst 33342 to prevent ESX binding to the HER2/*neu* promoter. ***B***, EMSAs were performed for each agent and the percent inhibition of complex formation was determined by comparing the ESX/DNA complex of drug treated samples to the average complex of 3 untreated controls. The percent inhibition of complex formation was averaged from a minimum of 3 separate experiments and plotted against drug concentration (μM). *Bars*, SD. The IC_{50} values (the amount of drug required to inhibit complex formation by 50%) are summarized in Table 1.

Figure 3: Inhibition of cell-free transcription from the HER2/*neu* promoter by Hoechst 33342. Hoechst 33342 was incubated with linearized plasmid DNA containing the HER2/*neu* promoter followed by incubation with SK-Br-3 nuclear extract and labeling cocktail, as described in Methods. Samples were loaded onto a 7 M-urea polyacrylamide gel, electrophoresed, dried, and exposed to PhosphorImaging Screen with ^{32}P signal quantitated by ImageQuant software. Normalization for equal loading was based on an internal control (IC). The following is a representative cell-free transcription assay showing the concentration-dependent inhibition of HER2/*neu* transcript formation by Hoechst 33342. *Lanes 1, 6, and 7* are untreated controls. *Lanes 2-5* are Hoechst 33342 treatment at 10.0, 5.0, 2.5 and 1.25 μM, respectively. An RNA

ladder was used to verify the band of interest based on transcript size, ~760 base pairs, as noted on the scale to the right.

Figure 4: Inhibition of HER2/*neu* promoter transcript expression by each DNA-binding agent. For each DNA binding agent, cell-free transcription assays were performed and the percent inhibition of transcript formation was determined by comparing the normalized HER2/*neu* transcript signal of drug-treated samples with the average normalized HER2/*neu* transcript signal of 4 untreated controls. The percent inhibition of transcript formation was averaged from 3-4 experiments and plotted against drug concentration (μM). *Bars*, SD.

Figure 5: Inhibition of HER2/*neu* cellular mRNA levels in SK-Br-3 cells by DNA-binding agents. ***A***, SK-Br-3 cells were exposed to Hoechst 33342 for 24 hours at the indicated concentrations followed by harvesting total RNA. Samples were electrophoresed on a formaldehyde-agarose gel, transferred to nylon membrane and probed with GAPDH and HER2/*neu* ^{32}P-labeled cDNAs. Shown is a representative northern blot demonstrating a concentration-dependent decrease in HER2/*neu* and GAPDH mRNA signals produced by Hoechst 33342. *Lanes 1, 2, 7 and 8* are untreated controls, *Lanes 3-6* are Hoechst 33342 treatments at 10, 5.0, 2.5 and 1.0 μM, respectively. ***B***, Northern blot analysis of cells treated 24 hours with each agent was performed and the percent inhibition of mRNA production determined for both HER2/*neu* (■) and GAPDH (◪). Comparison of the drug treated HER2/*neu* signal to the average HER2/*neu* signal of 4 untreated controls yielded percent inhibition of mRNA production. The results were averaged from a minimum of 2 experiments with duplicate samples and plotted against drug concentration. Additionally, northern blot analysis was performed after continuous 50 μM distamycin treatment of SK-Br-3 cells for 24, 48 and 72 hours. Comparison of distamycin-treated mRNA signal to the average signal generated by 4 untreated controls yielded percent inhibition HER2/*neu* and GAPDH mRNA production. The results of 6 separate studies were plotted against time. GAPDH mRNA was used in this study as a measure of general transcription versus HER2/*neu* mRNA as the drug-targeted site of transcription. Equal loading was verified by visual inspection on a UV light box. For some data points error bars were

not included since RNA recovery made it difficult to obtain consistent data. The difficulty occurred because the drug was relatively cytotoxic under the conditions studied. *Bars*, SD.

Figure 1

A.

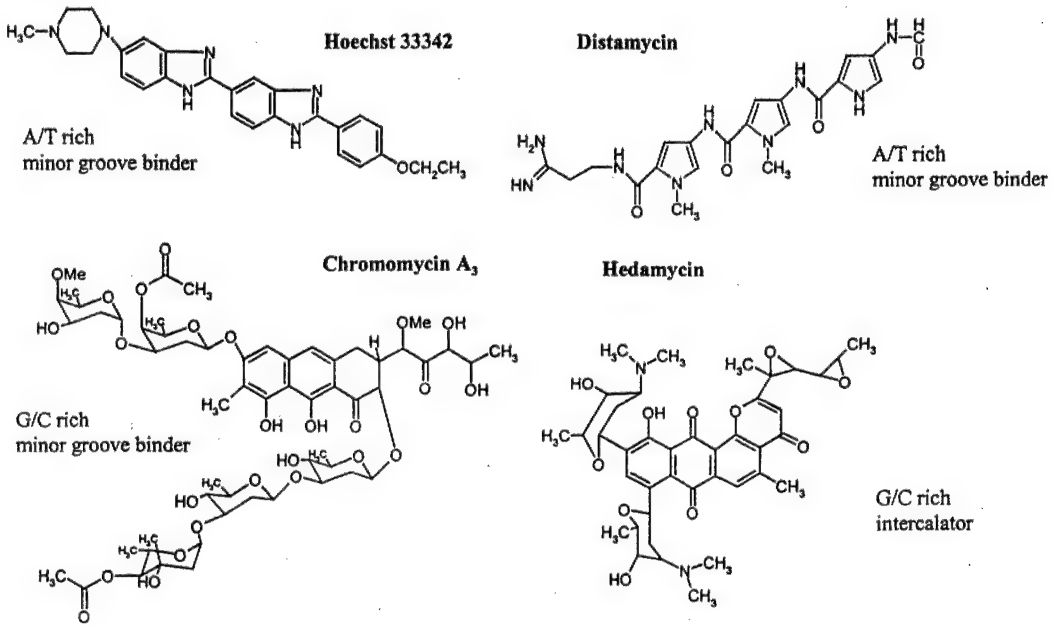
Hoechst 33342
A/T rich
minor groove binder
Distamycin
A/T rich
minor groove binder
Chromomycin A3
G/C rich
minor groove binder
Hedamycin
G/C rich
intercalator

B.

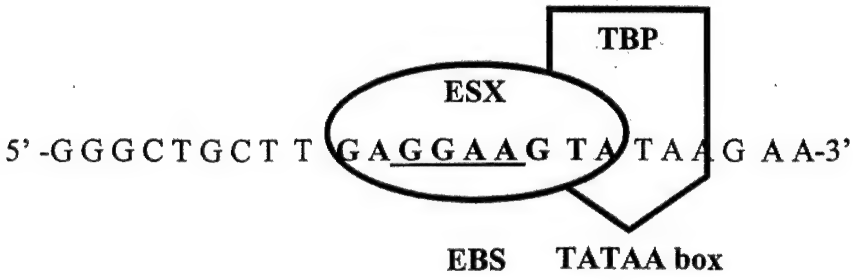
TBP
ESX
5'-GGGCTGCTT GAGGAAG TATAAG AA-3'
EBS
TATAA box

Figure 2

A.

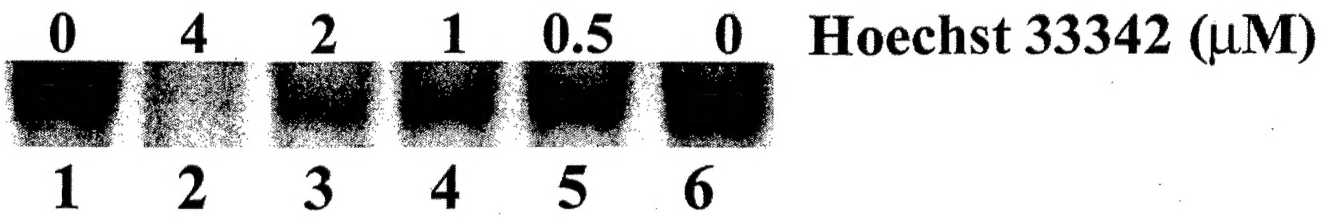
0
4
2
1
0.5
0
Hoechst 33342 (μM)
1
2
3
4
5
6

B.

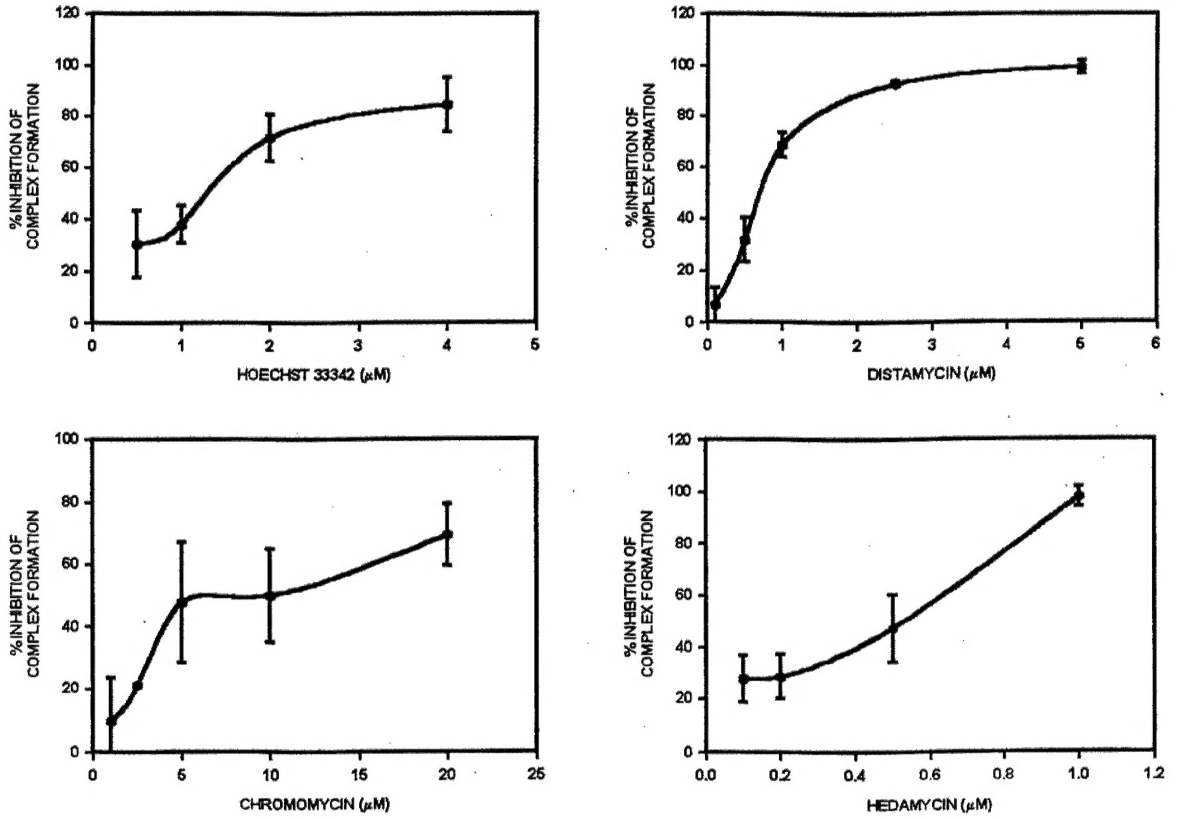
% INHIBITION OF COMPLEX FORMATION
HOECHST 33342 (μM)
DISTAMYCIN (μM)
CHROMOMYCIN (μM)
HEDAMYCIN (μM)

Figure 3

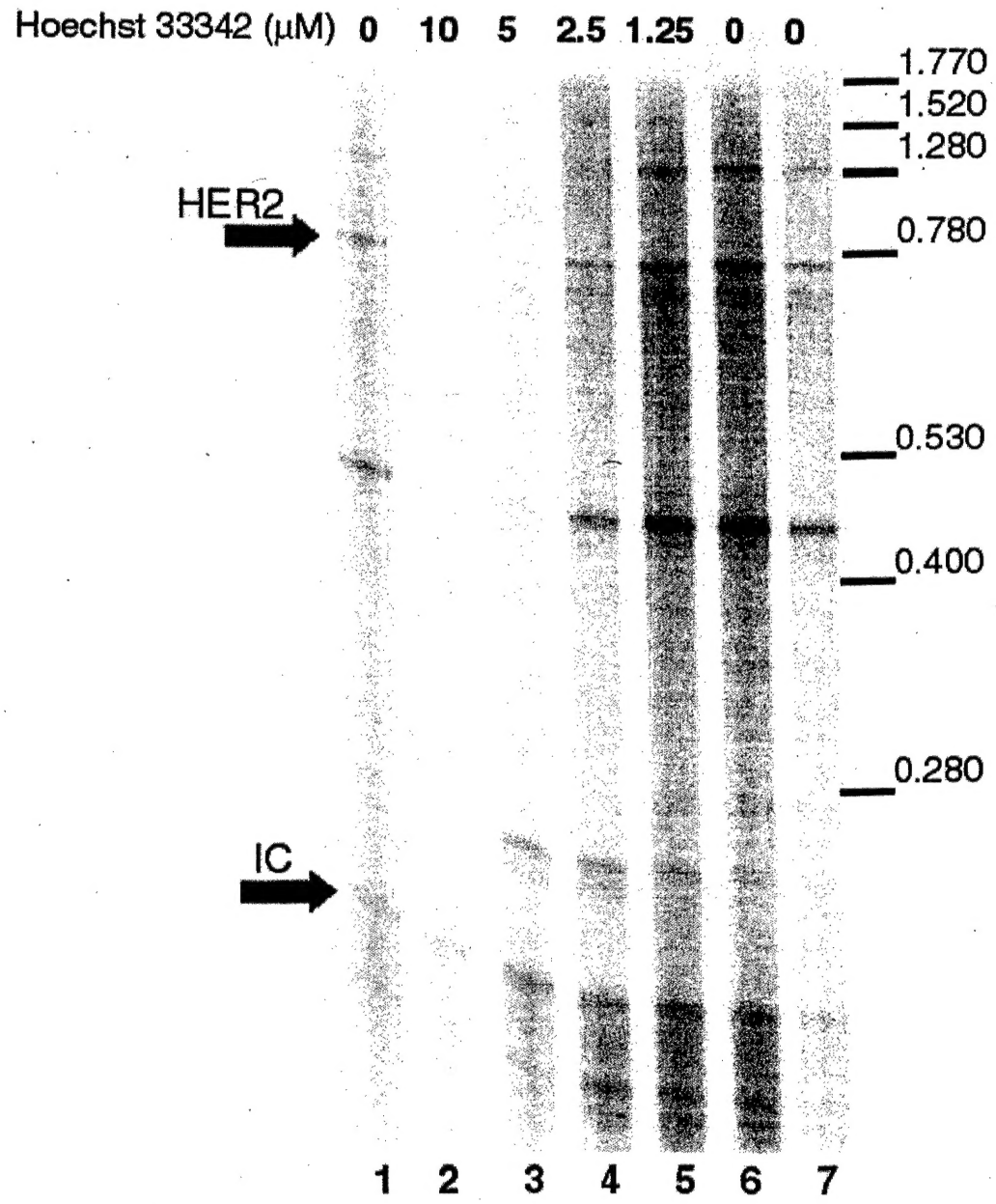
Hoechst 33342 (μM) 0 10 5 2.5 1.25 0 0
1.770
1.520
1.280
0.780
0.530
0.400
0.280
HER2
IC
1 2 3 4 5 6 7

Figure 4

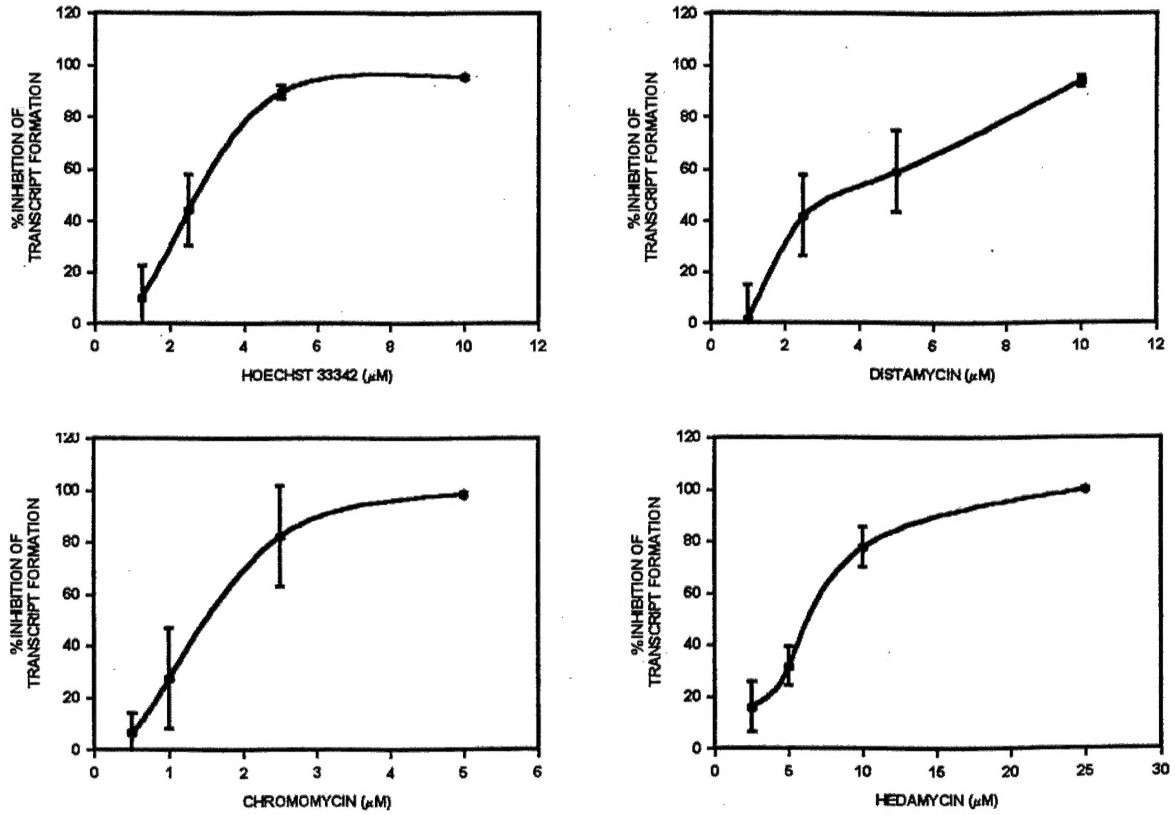
%INHIBITION OF TRANSCRIPT FORMATION
HOECHST 33342 (μM)
DISTAMYCIN (μM)
CHROMOMYCIN (μM)
HEDAMYCIN (μM)

Figure 5

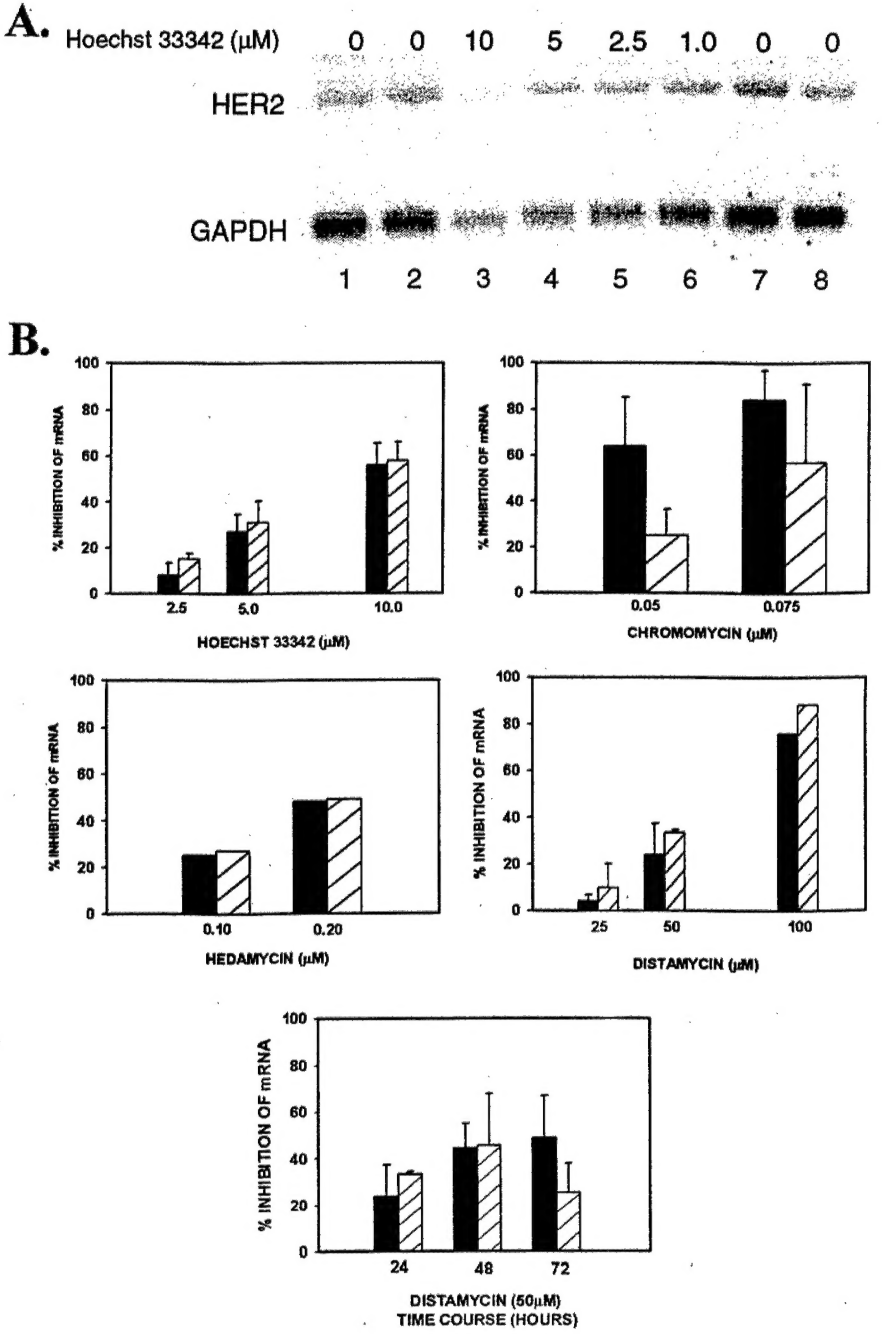
A.
Hoechst 33342 (μM)
0 0 10 5 2.5 1.0 0 0
HER2
GAPDH
1 2 3 4 5 6 7 8
B.
% INHIBITION OF mRNA
HOECHST 33342 (μM)
2.5 5.0 10.0
CHROMOMYCIN (μM)
0.05 0.075
HEDAMYCIN (μM)
0.10 0.20
DISTAMYCIN (μM)
25 50 100
DISTAMYCIN (50μM)
TIME COURSE (HOURS)
24 48 72